DEPARTMENT OF OCEAN ENGINEERING
MASSACHUSETTS INSTITUTE OF TECHNOLOGY
CAMBRIDGE, MASSACHUSETTS 02139

PRELIMINARY MECHANICAL REDESIGN OF AN EXISTING GAS-TURBINE ENGINE TO INCORPORATE A HIGH-EFFICIENCY, LOW-PRESSURE-RATIO, HIGHLY-REGENERATIVE CYCLE FOR MARINE APPLICATIONS

by
PATRICK KEVIN POOLE
and
LEO DENNIS OWENS, JR.

XIII-A JUNE 1984

PRELIMINARY MECHANICAL REDESIGN OF AN EXISTING GAS-TURBINE ENGINE TO INCORPORATE A HIGH-EFFICIENCY, LOW-PRESSURE-RATIO, HIGHLY-REGENERATIVE CYCLE FOR MARINE APPLICATIONS

by
PATRICK KEVIN POOLE
BSEE, University of Louisville (1976)
and
LEO DENNIS OWENS, JR.
BSCHE, Purdue University (1978)

SUBMITTED TO THE DEPARTMENT OF
OCEAN ENGINEERING
IN PARTIAL FULFILLMENT OF THE
REQUIREMENTS OF THE
DEGREES OF

MASTER OF SCIENCE IN NAVAL ARCHITECTURE AND MARINE ENGINEERING
AND MASTER OF SCIENCE IN MECHANICAL ENGINEERING

at the
MASSACHUSETTS INSTITUTE OF TECHNOLOGY
JUNE 1984

PRELIMINARY MECHANICAL REDESIGN OF AN EXISTING GAS-TURBINE ENGINE TO INCORPORATE A HIGH-EFFICIENCY, LOW-PRESSURE-RATIO, HIGHLY-REGENERATIVE CYCLE FOR MARINE APPLICATIONS

by
PATRICK KEVIN POOLE
and
LEO DENNIS OWENS, JR.

Submitted to the Departments of Ocean and Mechanical Engineering on May 11, 1984 in partial fulfillment of the requirements for the Degrees of Master of Science in Naval Architecture and Marine Engineering and Master of Science in Mechanical Engineering

ABSTRACT

The low-pressure-ratio, highly-regenerative, gas-turbine engine has been proposed as an efficient alternative to other current small-scale marine propulsion systems. This paper provides a preliminary mechanical redesign of an existing gas-turbine engine to lower the compressor pressure ratio and incorporate a regenerator. One basic design is presented with several alternative turbine modifications.

The redesign includes elimination of the second stage of the original two-stage centrifugal compressor, increasing the liner flow area of the existing annular combustor, elimination of the first stage of the three-stage axial turbine, reblading the last two turbine stages, sizing an appropriate regenerator, and designing annular inlet and outlet scrolls to direct gas flow to the regenerator.

Due to the simplicity of the original engine and its operating environment (high-altitude turboprop), modification to a regenerative system for marine use appears feasible and attractive. The redesigned engine has a maximum design-point thermal efficiency of 49 percent with a reduction in power output from the original engine of only 12.5 percent. The extent of the modifications to the original engine could be reduced somewhat to enhance economic attractiveness at the expense of reduced efficiency or power output.

Thesis Supervisor: David Gordon Wilson
Title: Professor of Mechanical Engineering

TABLE OF CONTENTS

NOMENCLATURE

A	area
A_{ref}	maximum cross-sectional area of combustor casing in the absence of a liner
b	blade axial chord
c	blade chord
C	absolute velocity
C_p	specific heat at constant pressure
e	blade surface curvature
Δh	change in enthalpy
$\dot{m}$	mass flow rate
M	Mach number
o	blade-throat width
P	pressure
ΔP_L	combustor liner pressure drop
r	radius
R_n	turbine stage reaction
s	turbine blade spacing
t	thickness
T	absolute temperature
u	blade speed
w	relative velocity
z	number of blades per disk (turbine nozzle or rotor)
α	angle between absolute velocity vector and axial direction
β	angle between relative velocity vector and axial direction
ρ	density

SUBSCRIPTS

o	stagnation property of gas
1	turbine rotor inlet value
2	turbine rotor outlet value
3	combustor inlet value
a	annulus value
NE	nozzle exit value
NI	nozzle inlet value
p	combustion products
st	static property of gas
te	turbine-blade trailing-edge value
θ	tangential value
x	axial value

LIST OF TABLES

LIST OF FIGURES

I. INTRODUCTION

The redesign attempted in this work follows the thermodynamic analysis of the selected engine presented by King (1). That investigation concluded that the thermal efficiency could be greatly increased by reducing the pressure ratio to allow incorporation of a rotary regenerator by eliminating the second-stage centrifugal compressor and by designing a new turbine section utilizing ceramic materials. A summary of the thermodynamic analysis for a regenerative cycle can be seen in figure 1 as a plot of thermal efficiency versus specific power. The elimnation of the second-stage radial compressor results in a total-pressure ratio of approximately 4.3. If we assume, for preliminary investigation, that the original-configuration turbine first-stage rotor-inlet temperature of 1381 K is maintained, then a total-temperature ratio of 4.8 is estimated. From figure 1, a thermal efficiency of fifty percent (near optimal) with a specific power of approximately .75 is expected. These results are based on a cycle analysis for the specific values of regenerator effectiveness, compressor and expander polytropic efficiency, and pressure losses expected in the cycle. The performance calculated by King for the selected engine, after modification, closely follows these predictions.

It is expected that some degradation in compressor and expander efficiencies will occur due to the modification of the engine and also due to possible increased losses resulting from the modified operating

environment of a sea-going vessel. However, a thermal efficiency of forty-five to forty-nine percent still seems achievable.

King's recommendation that a new turbine be substituted rather than trying to modify the original components was made based upon the significant decrease in turbine inlet static gas density caused by the pressure reduction. Reducing the pressure ratio by eliminating the second-stage centrifugal compressor and operating the original first stage at its design speed allows the turbine to maintain the original mass flow rate, but at a much higher axial velocity. This fact is advantageous in terms of keeping power output high but disadvantageous when losses and possible choked flow are considered. The decrease in static density is approximately 60 percent and can be compensated for somewhat in the turbine section through an increase in the annulus area. In the combustor, however, such density decrease may require total component replacement unless the original design was significantly oversized. In all cases, the proposed modification must account for this increased axial velocity. One alternative not addressed in this preliminary redesign is a decrease in the engine mass flow caused by a reduction in the compressor rotor flow area. This method would compensate for the decreased static density, thereby allowing engine operation with very little combustor and turbine modification but it would also result in a significant decrease in power output. Because of this latter consequence, this alternative is not considered attractive from a power-versus-acquisition-cost aspect.

Since the selected turbine is a relatively uncomplicated, single-shaft, fixed-geometry component, we felt strongly that it could be modified through blade changes, stage relocation, etc., while utilizing the original shroud dimensions. This latter restraint set the bounds for the turbine design task. The combustor investigation involved verification that the unit was sufficiently overdesigned in the original configuration to successfully handle the increase in volume flow rate. This was a "go-no go" situation where an insufficiency would cause complete replacement of the component and subsequent modification of the turbine casing. The regenerator, scroll and ducting design were based primarily on sizing requirements to provide the necessary gas velocities and heat-transfer rates. The physical arrangement of the engine and its components, in particular the regenerator system, was selected to enhance ease of installation and maintenance accessability in an existing fishing vessel engine room.

The engine chosen for modification is the GARRETT T76-420/421, which is an upgraded military version of the TPE 331. These power plants are used primarily in naval turboprop aircraft.

FIGURE 1

THERMAL EFFICIENCY VERSUS SPECIFIC POWER FOR A REGENERATIVE CYCLE

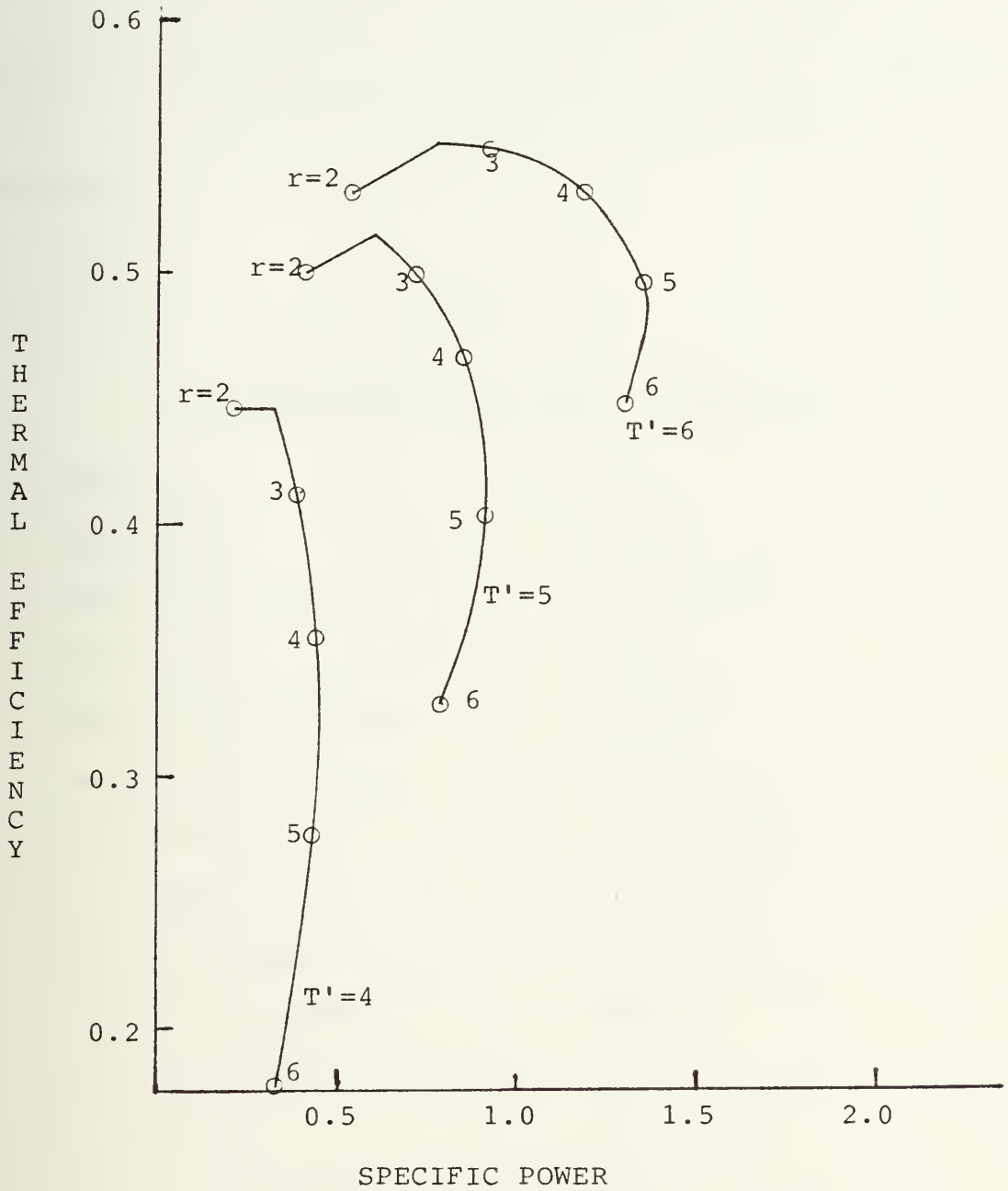

$$r = \frac{\text{Compressor outlet total pressure}}{\text{Compressor inlet total pressure}}$$

$$T' = \frac{\text{Turbine inlet total temperature}}{\text{Compressor inlet total temperature}}$$

II. COMBUSTOR

The existing combustor is a reverse-flow annular type with original specifications and operating characteristics as stipulated in table 1. This information was graciously provided by Garrett AiResearch.

TABLE 1

COMBUSTOR SPECIFICATIONS AND CHARACTERISTICS

Burner Length	0.137 m.
Burner Volume	0.00595 cu.m.
Burner Surface Area	0.314 sq. m.
Channel Height	0.043 m.
Combustion System Volume	0.008 cu.m.
Transition Liner Volume	0.002 cu.m.
Fuel Flow Rate	0.073 kg/sec.
Air Flow Rate	3.15 kg/sec.
Inlet Total Pressure	1081.5 kPa
Inlet Total Temperature	633 K
Outlet Total Temperature (ave.)	1381.5 K
Pattern Factor	0.2
Combustor Efficiency	99%
Total-Pressure Loss	2.5%

In keeping with our overall design philosophy, we would prefer to use the existing combustor in the modified engine, thereby reducing conversion cost. A cursory inspection of the new operating conditions listed in table 2 leads to the conclusion that this will be impossible due to the large decrease in inlet gas density and the corresponding increase in gas velocities and pressure losses.

TABLE 2

MODIFIED COMBUSTOR OPERATING CONDITIONS

Fuel Flow Rate	0.0366 kg/sec.
Air Flow Rate	3.197 kg/sec.
Inlet Total Pressure	422.8 kPa
Inlet Total Temperature	1011.6 K
Outlet Total Temperature	1381.5 K

However, the economic attractiveness of utilizing the original combustor is so strong that a more careful analysis is proposed. The new operating conditions would certainly impose greater pressure losses due to reduced aerodynamic performance of the chamber in general and in particular to increased losses in the inlet annular diffuser. But as long as the flow is led to the diffuser without excessive swirl, this penalty can be sustained while still salvaging the combustor. To assess the feasibility of retaining the present combustor, three parameters will be examined: inlet Mach number, liner jet penetration and required Heat Release Rate (2). For a

positive determination to be made concerning the combustor, the inlet Mach number must remain below 0.7 (3), the liner jet penetration must remain approximately constant and the Heat Release Rate must remain constant or decrease.

The original inlet Mach number of 0.115 is well below our operating criterion and is indicative of the original engine design objective of being able to successfully relight after flameout at an altitude of twenty-thousand feet. For the modified-engine operating conditions the inlet Mach number is 0.407, which is still well below our operating limit.

To ensure that the jet penetration remains the same, the momentum flux ratio must be held constant. This is the ratio of the jet value of the product of gas density with the gas velocity squared, to the inner-liner value of the same product. One way to accomplish this without drastic modifications is to increase the flow area of the liner by increasing the jet and swirl vane sizes. Using the development of Lefebvre (2) and specifying a ten percent reduction in chamber aerodynamic performance, the jet diameter ratio of the modified to the original design is 2.48.

Finally, the required Heat Release Rates of the original and modified combustors must be compared. Again from Lefebvre (2,4), the parameter to be utilized for this comparison is dependent upon the chamber mixing rate and is computed as follows:

$$\text{Heat Release Criterion} = \left(\frac{P_3 \quad A_{ref}}{\dot{m}_A \quad T_3^{\frac{1}{2}}} \right) \left(\frac{\Delta P_L}{P_3} \right)^{\frac{1}{2}}$$

By conservatively specifying that the modified-combustor relative pressure loss is twice that of the original design, we have calculated that the modification has decreased the thermodynamic loading by sixty percent.

Since all three of our proposed criteria have been met or favorably exceeded, we recommend that the existing combustor be utilized with the existing liner jet diameters increased by a factor of 2.5. It is worthy to note here that, to date, the most effective and reliable method of assessing a combustor's ability to function in a given engine is to place it on the test stand in an appropriate set of operating conditions and note where holes are burned through the liner (2). The type of information that can be obtained in this manner is indispensible to the combustor designer, and we heartily recommend a similar treatment for this combuster at the detailed design level.

III. TURBINE ANALYSIS

GENERAL DISCUSSION

The reduction in pressure at the turbine inlet of the redesigned configuration requires an increase in either annulus area or axial velocity or both, since the mass flow is the same as the original design. An area increase is obtained by removing the first and second stages and designing a new first stage for the old second-stage location. Utilization of the existing first-stage hub in the new first stage is possible since the rotor blades are attached by a "fir tree" coupling and can be easily removed and replaced. The existing third-stage location is now the new second-stage position. Since the third stage has integrally cast hub and blades, two proposals are made and presented:

(1) to grind back the nozzle and rotor-blade trailing edges such that appropriate exit angles are achieved, and

(2) to manufacture a completely new second stage, including hub, nozzles and rotor blades.

In order to reduce the scope of the investigation and maintain one first-stage design for both proposals, the modification was restricted by matching the first and second stages through utilization of the inlet angle of the existing third-stage nozzle. This restriction defined the first-stage outlet angle and allowed the possible utilization of the existing third-stage nozzle as the new second-stage nozzle. The investigation of this possibility is

accomplished analytically to determine the extent of reduction of axial chord in the nozzle. Similarly, the same method is used to determine the reduction necessary in the third-stage rotor axial chord for utilization as the redesigned second-stage rotor (proposal 1). Additionally, new blade shapes for the second stage based on the same nozzle inlet angle are provided (proposal 2).

The first-stage inlet temperature is maintained to that of the original design (1381.5 K). The first-stage outlet temperature is specified at 1190 K to limit the necessity for blade cooling to the first stage. Since the first-stage hub is used in the new design, it is anticipated that the original first-stage blade and hub cooling-pattern would be appropriate for the modified version. This appears feasible since the original pattern was adapted from the GARRETT TPE 731-3 engine.

ORIGINAL-CONFIGURATION ANALYSIS

From the data and technical drawings provided by GARRETT and from the results of King's thermodynamic analysis listed in table 3, the parameters for the stations identified in figure 2 are derived (table 4). Utilizing these values, an estimation of the original third-stage blade shapes was made. This estimate is based on three assumptions and calculations from four equations. The assumptions are:

(1) third-stage exit velocity is axial;

(2) second-stage reaction at mean radius is 50 percent; and

(3) the tangential velocity between any set of nozzle and rotor blades is constant.

The four equations utilized throughout the design process are:

(1) $$\Delta h_{o_{stage}} = \frac{1}{g_c} (u_2 C_{\theta_2} - u_1 C_{\theta_1})$$

(2) $$R_n \equiv \frac{\Delta h_{st}}{\Delta h_o} = 1 - \frac{C_2^2 - C_1^2}{2(u_2 C_{\theta_2} - u_1 C_{\theta_1})}$$

(3) $$\dot{m}_{in} = (\rho_{st} A_a C_x)_{in}$$

(4) $$\dot{m}_{out} = (\rho_{st} A_a C_x)_{out}$$

Combining these assumptions and equations with the data in table 4, the velocity diagrams for the existing third stage can be determined. Additionally, by further assuming that there is constant specific work and constant axial velocity (Free-Vortex Design) at all radial blade positions, the hub and tip velocity diagrams can also be determined (figure 3). Specific values of velocities labeled in the above figure may be found in table 5.

TABLE 3

ORIGINAL CONFIGURATION CYCLE DATA AT DESIGN POINT

Compressor	
Inlet total pressure (kPa)	101.325
Inlet total temperature (K)	288.15
Inlet mass flow (kg/sec)	3.4732
Rotor speed (rpm)	41,730
Total-pressure ratio	10.674
Total-temperature ratio	2.1818
Total-to-total isentropic efficiency	0.7904
Total-to-total polytropic efficiency	0.8454
Combustor	
Inlet total pressure (kPa)	1081.5
Inlet total temperature (K)	628.6
Inlet mass flow (kg/sec)	3.2961
Fuel flow (kg/sec)	0.0725
Pressure loss (%)	0.045
Efficiency of combustion	0.996
Exit total temperature (K)	1381.5
Turbine	
Inlet total pressure (kPa)	1032.9
Inlet total temperature (K)	1381.5
Inlet mass flow (kg/sec)	3.3686
Total-to-static pressure ratio	10.194

Total-to-total temperature ratio	1.5649
Exit total temperature (K)	882.8
Exit static pressure (kPa)	101.325
Total-to-static isentropic efficiency	0.8630
Total-to-static polytropic efficiency	0.8256
Cycle and mechanical values	
Turbine-cooling-air mass flow (kg/sec)	0.1389
Leakage mass flow (kg/sec)	0.0381
Mechanical losses (kW)	9.4
Gearbox efficiency	0.9796
Engine performance	
Power output (kW)	799.0
Specific power	0.7957
Thermal efficiency	0.2734
Specific fuel consumption (kg/kW-hr)	0.3268

TABLE 4

ORIGINAL-CONFIGURATION PARAMETERS

STATION	1	2	3	4	5	6	7
P (kPa)	1032.8	1004.6	481.9	461.9	226.1	219.3	110.0
T_o (K)	1435.6	1381.5	1188.9	1188.9	1016.7	1016.7	872.8
Cp (J/kg-K)	1210	1210	1183	1183	1153	1153	1131
A_a (sq.m.)*	-	.0094	.00935	.0175	.0219	.03165	.03545
r_m (m)	-	.0832	.0836	.0897	.0922	.09705	.0983

* A_a at Rotor Mean Radius (r_m)

FIGURE 2

ORIGINAL-CONFIGURATION STATION LOCATIONS

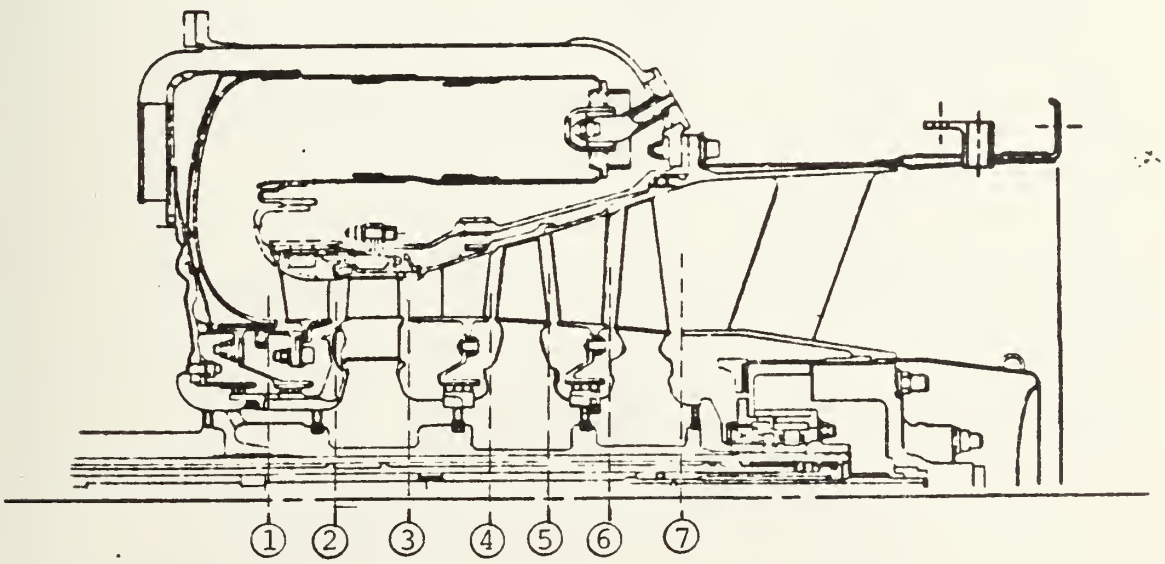

FIGURE 3

ORIGINAL CONFIGURATION STAGE - THREE

HUB - MEAN - TIP

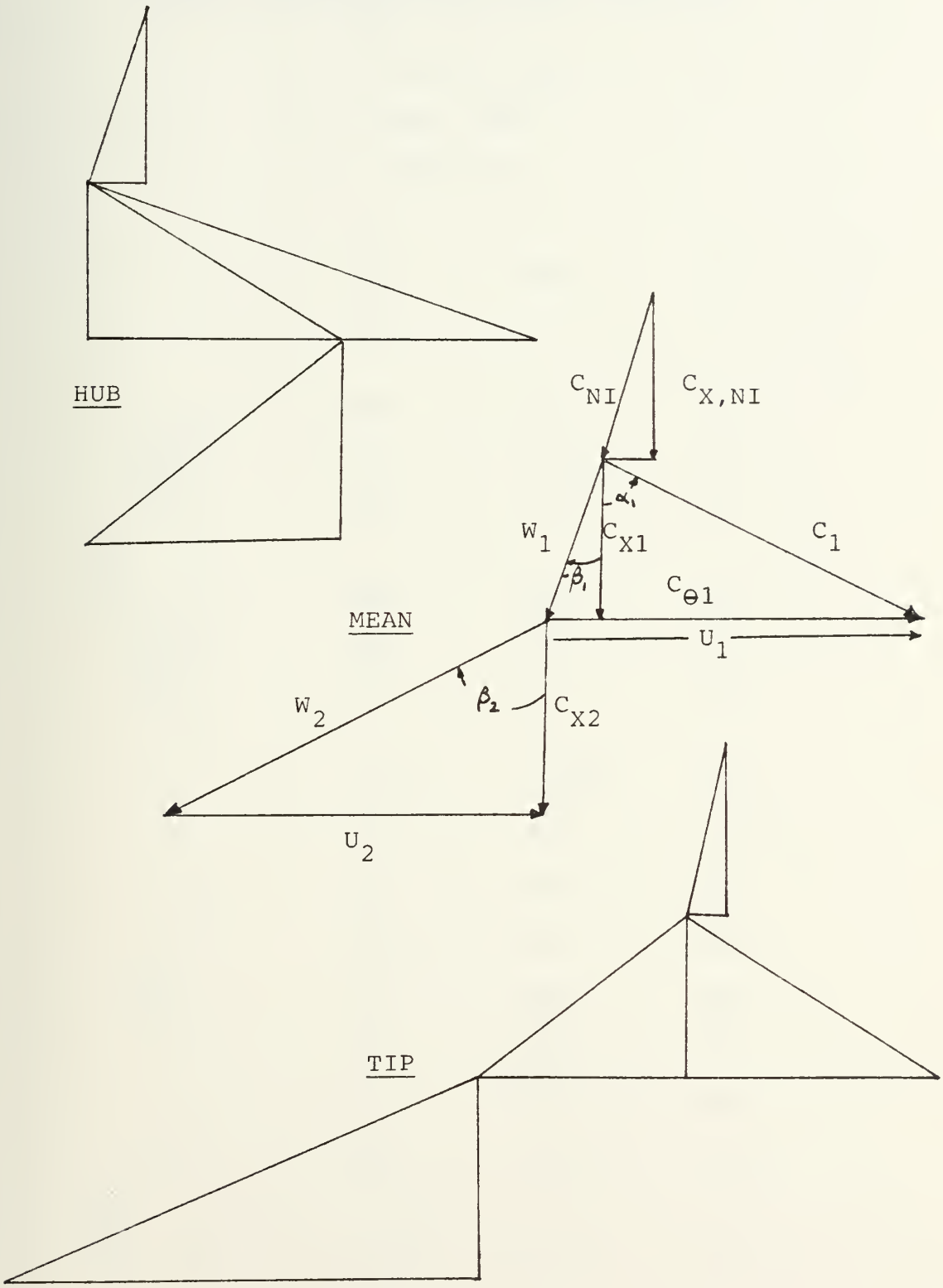

TABLE 5

ORIGINAL CONFIGURATION STAGE-THREE VELOCITIES

velocity (m/s)

angle (deg)

radius (m)

			HUB	MEAN	TIP
NOZZLE	inlet	$C_{x_{NI}}$	203	203	203
		C_{NI}	215	210.5	208
		α_{NI}	-19	-15.4	-13
	outlet	$C_{x_{NE}}$	209	209	209
		C_{NE}	574	444	373
		α_{NE}	68.7	61.9	55.9
ROTOR	inlet	r_1	.0711	.09705	.123
		u_1	311	424	537.5
		C_{x_1}	180	180	180
		C_1	564.5	431	357.5
		C_{θ_1}	535	392	309
		w_1	359	183	291
		α_1	71.4	65.3	59.8
		β_1	59.9	-10.5	-51.8
		r_2	.0696	.0983	.127

outlet	u_2	304	430	555
	C_{x_2}	230	230	230
	C_2	230	230	230
	C_{θ_2}	0	0	0
	w_2	381.5	488	601
	α_2	0	0	0
	β_2	58.9	61.9	67.5
	R_n	0.20	0.60	0.77

The original third-stage velocity diagrams were determined to enable their use in a later analysis to investigate the feasibility of utilizing a modified third stage as the new second stage (proposal 1). We found that the original configuration is not a constant-axial-velocity design. The axial velocity decreases over the length of the turbine as the annulus area increases at a faster rate than that of the density decrease. Because of this, separate inlet and outlet velocity diagrams (vs. simple velocity diagrams) are used. The conventions described by Carmichael are used throughout (5).

REDESIGNED-CONFIGURATION ANALYSIS

The initial effort in the redesigned-configuration analysis was to determine the velocity diagrams for the new first and second stages. Physical measurements from technical drawings provided the annulus areas for each stage. As stated earlier, the inlet angle of the second-stage nozzle was held constant from the original third-stage design. The polytropic total-total efficiency of the existing third stage is calculated at 89.5 percent. Since it is hoped that this stage can be modified by grinding back the trailing edges of both the nozzle and rotor, a reduction of efficiency for this stage to 88 percent (polytropic, total-total) was assumed.

The increase in annulus area gained by moving the first stage back to the original second-stage location only partially overcomes the effect on the change in inlet density caused by the reduction in pressure ratio. The remaining factor will be accounted for by an increase in axial velocity. The design of the new first stage is based upon the desired values of inlet/outlet temperature (1381.5 K/1190 K). As stated previously, the original first-stage hub and the nozzle-and rotor-blade axial-chord dimensions are used.

From the specified inlet and outlet temperatures and the work and flow coefficients of the first stage an estimation of polytropic total-total efficiency can be made based on plots given by both Wilson and Horlock (3,6). For calculated values of flow coefficient and work or loading coefficient of approximately 0.7 and 1.45, respectively, the estimated efficiency is 92 percent. The calculated flow

coefficient is near the optimum value for the given stage loading. The redesigned-configuration parameters for stations of interest (figure 4) were determined from the above data and the results are listed in table 6.

The same assumptions and equations used in the determination of the original third-stage design were utilized to arrive at the velocity diagrams for the modified design (figures 5 and 6). The specific velocity values are found in table 7 and 8, respectively.

TABLE 6

REDESIGNED-CONFIGURATION PARAMETERS

STATION	1	2	3	4	5
P (kPa)	403.8	391.7	203.0	197.0	111.3
T_o (K)	1430	1381.5	1190	1190	1052
Cpp (J/Kg-K)	-	1217	1217	1187	1187
A_a (sq.m.)*	-	.0155	.01973	.03165	.03545
r_m (m)	-	.09195	.09093	.09705	.0983

* A_a at Rotor Mean Radius (r_m)

FIGURE 4

REDESIGNED-CONFIGURATION STATION LOCATIONS

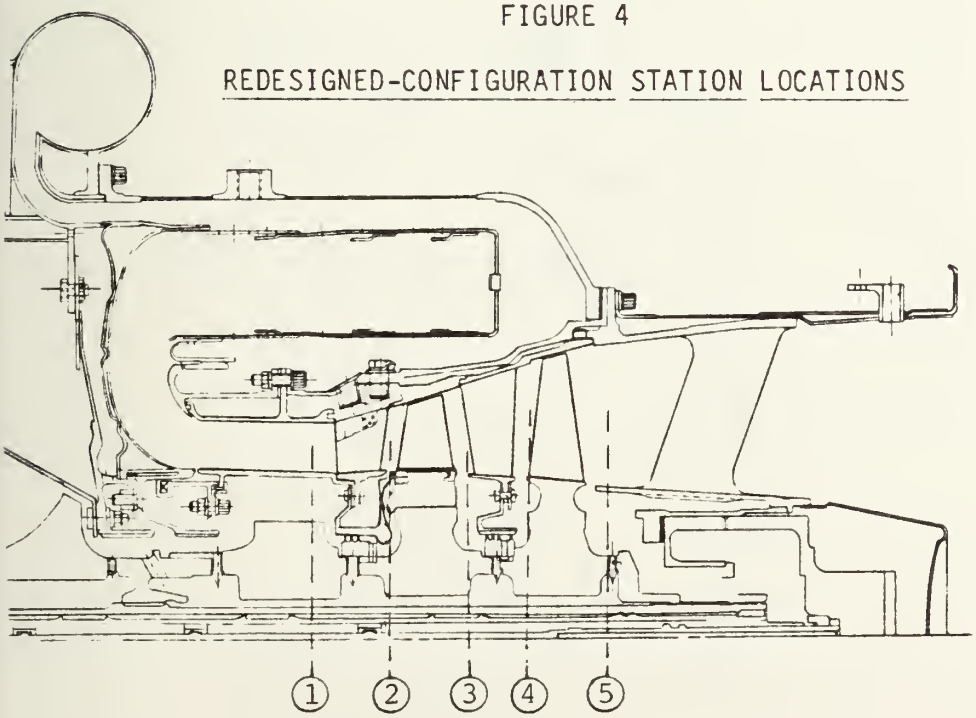

FIGURE 5

REDESIGNED CONFIGURATION STAGE - ONE

HUB - TIP - MEAN

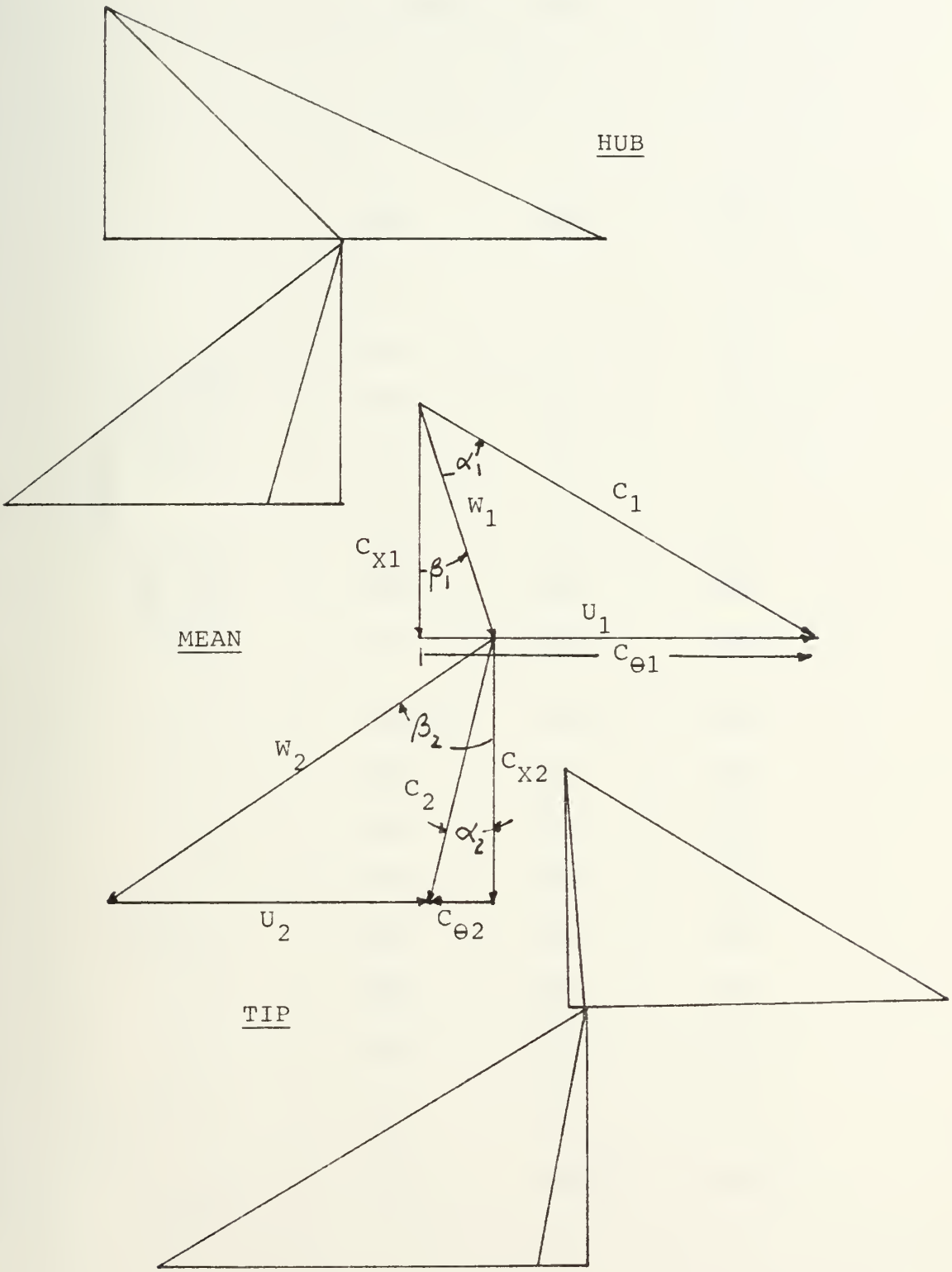

TABLE 7

REDESIGNED CONFIGURATION STAGE-ONE

velocity (m/s)

angle (deg)

radius (m)

			HUB	MEAN	TIP
NOZZLE	inlet	$C_{x_{NI}}$	310	310	310
		C_{NI}	310	310	310
		α_{NI}	0	0	0
	outlet	$C_{x_{NE}}$	305	305	305
		C_{NE}	696	590	548
		α_{NE}	64	58.9	56.2
ROTOR	inlet	r_1	.07417	.0920	.1021
		u_1	324	402	446
		C_{x_1}	300	300	300
		C_1	694	588	545
		C_{θ_1}	626	505	455
		w_1	426	353	300
		α_1	64.4	59.3	56.6
		β_1	45.2	19	1.7
		r_2	.0737	.09085	.1082

outlet			
u_2	322	397	473
C_{x_2}	330	330	330
C_2	343	339	336
C_{θ_2}	-93	-75.5	-63.5
w_2	530	338.5	630
α_2	15.8	12.9	10.9
β_2	51.5	55.1	58.4
R_n	0.22	0.505	0.605

FIGURE 6
REDESIGNED CONFIGURATION STAGE - TWO
HUB - TIP - MEAN

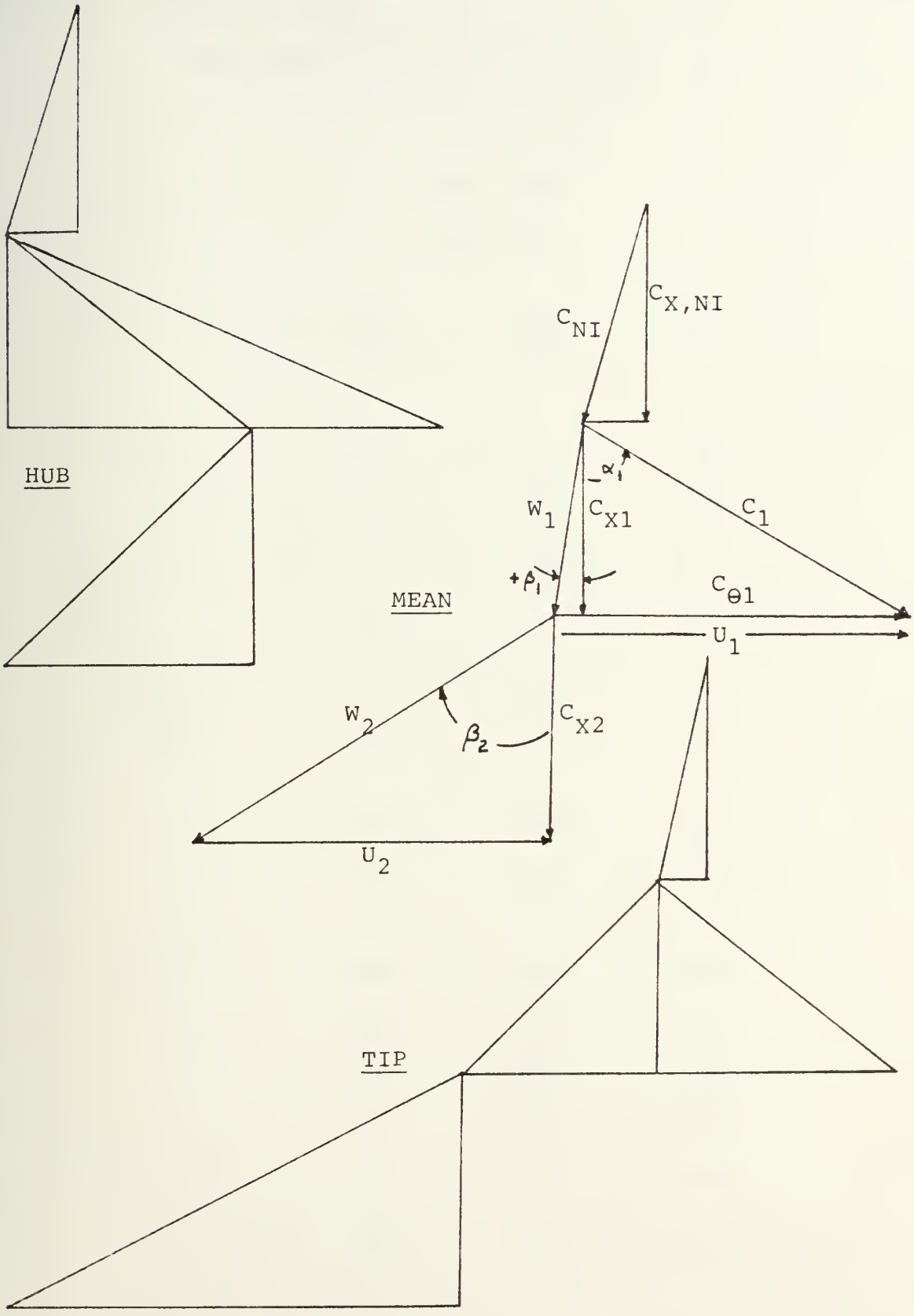

TABLE 8

REDESIGNED-CONFIGURATION STAGE-TWO

velocity (m/s)

angle (deg)

radius (m)

			HUB	MEAN	TIP
NOZZLE	inlet	$C_{x_{NI}}$	284	284	284
		C_{NI}	299	294	291
		α_{NI}	-18.1	-15.4	-12.6
	outlet	$C_{x_{NE}}$	271	271	271
		C_{NE}	593.5	472	401
		α_{NE}	62.8	55.0	47.5
		r_1	.0711	.09705	.123
		u_1	311	424	537.5
ROTOR	inlet	C_{x_1}	231	231	231
		C_1	576	450	375.5
		C_{θ_1}	528	387	296
		w_1	317	234	334
		α_1	66.4	59.1	52.0
		β_1	43.2	-9.1	-46.3
		r_2	.0696	.0983	.127

outlet	u_2	304	430	555
	C_{x_2}	282	282	282
	C_2	282	282	282
	C_{θ_2}	0	0	0
	w_2	415	514	622
	α_2	0	0	0
	β_2	47.2	56.7	63.1
	R_n	0.230	0.625	0.807

MODIFICATION OF EXISTING THIRD STAGE AS NEW SECOND STAGE

Since the velocity diagrams for the original- and redesigned-configuration last stages have similar exit angles, it may be possible to modify the original nozzle and rotor blades by grinding back the trailing edges until the desired exit angles are achieved as required by the velocity diagrams for the redesigned engine.

To make an analytical estimate of the feasibility of such modifications, it is first necessary to assume an existing blade shape. The method proposed by Wilson for preliminary design was utilized. The blade characteristics of the assumed nozzles and blades are presented in table 9, and figures 7 and 8 contain the assumed shapes. The indicated reductions in the axial chords are a result of the following analysis.

TABLE 9

ORIGINAL-CONFIGURATION STAGE-THREE

NOZZLE AND ROTOR CHARACTERISTICS

(MEAN RADIUS)

	Rotor (mm)	Nozzle (mm)
r	97.05	95.85
z	36	31
s	16.94	19.43
b	17.30	19.8
M_{throat}	.856	.745
s/e	0.425	0.50
o/s	0.464	0.463
Δt_{te}	0.847	0.970
e	39.90	38.90
o	7.86	9.0
c	27.94	21.72

FIGURE 7

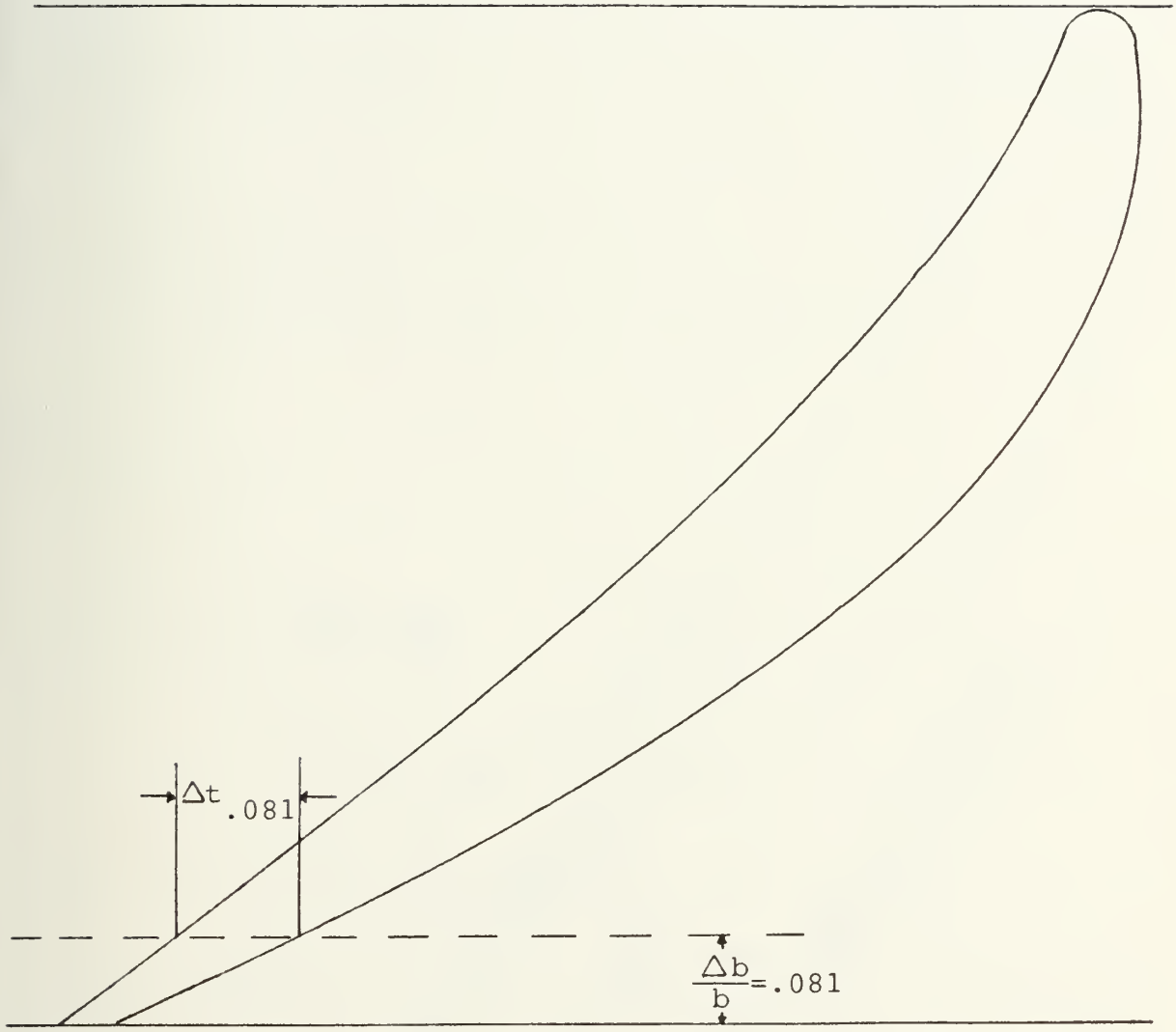

ORIGINAL CONFIGURATION STAGE - THREE ROTOR (MEAN RADIUS)

SCALE 7:1

FIGURE 8

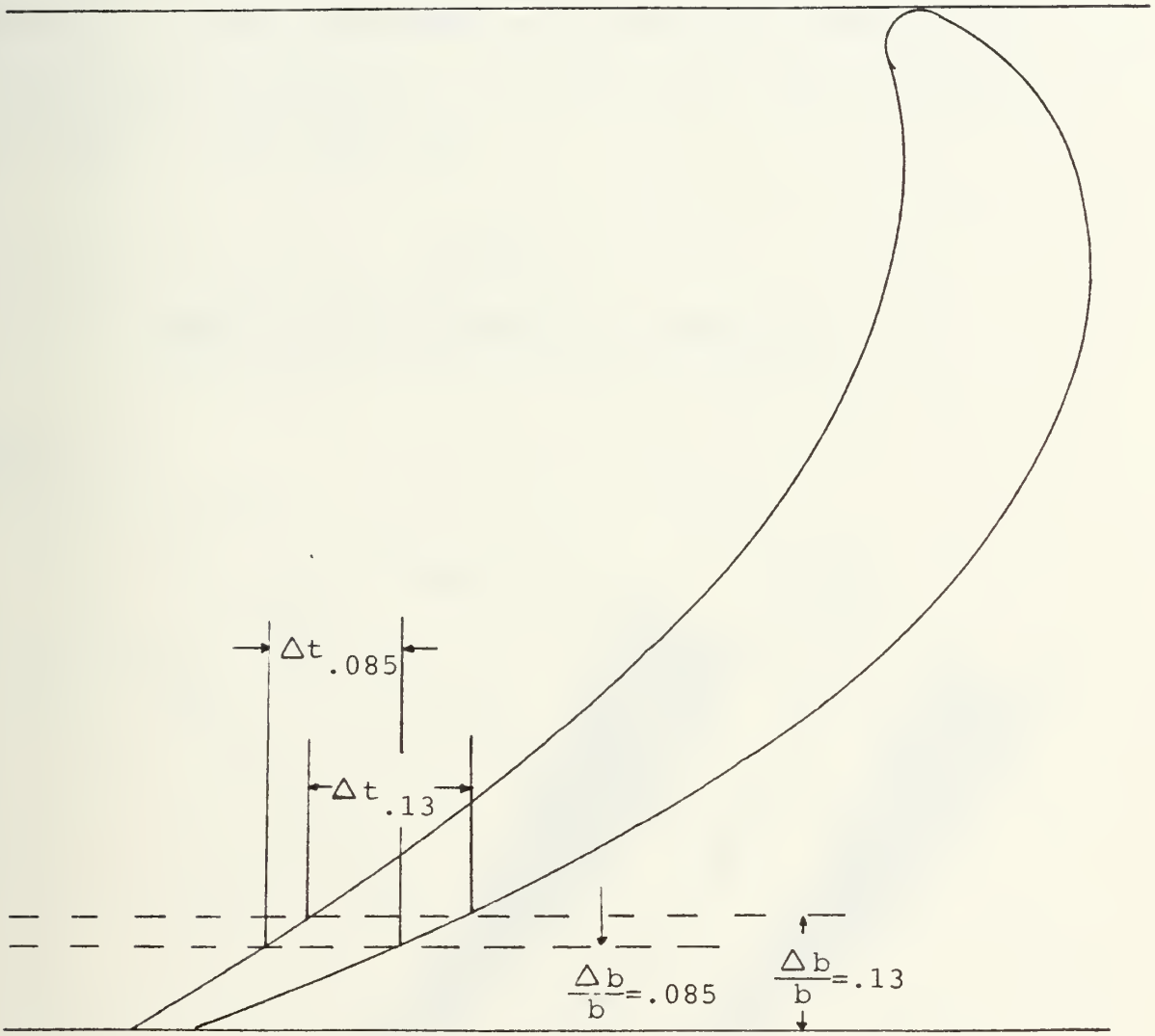

ORIGINIAL CONFIGURATION STAGE - THREE NOZZLE (MEAN RADIUS)

SCALE 8:1

ANALYTICAL MODEL FOR DETERMINING CHANGE IN AXIAL CHORD (b/b)

While using the method proposed by Wilson for blade shape design it was noticed that the tangent to a circle of radius e (blade surface curvature) gave an angle with the axial very close to that required by the velocity diagram for that blade. This occurred consistently, and so this phenomenon was incorporated into the proposed model as an assumption. The model also assumes that the mean flow stream at the last 15 percent of axial cord will follow a circular path of radius e + o/2, where o is the throat width.

FIGURE 9

ANALYTICAL MODEL PARAMETERS AND CONVENTION

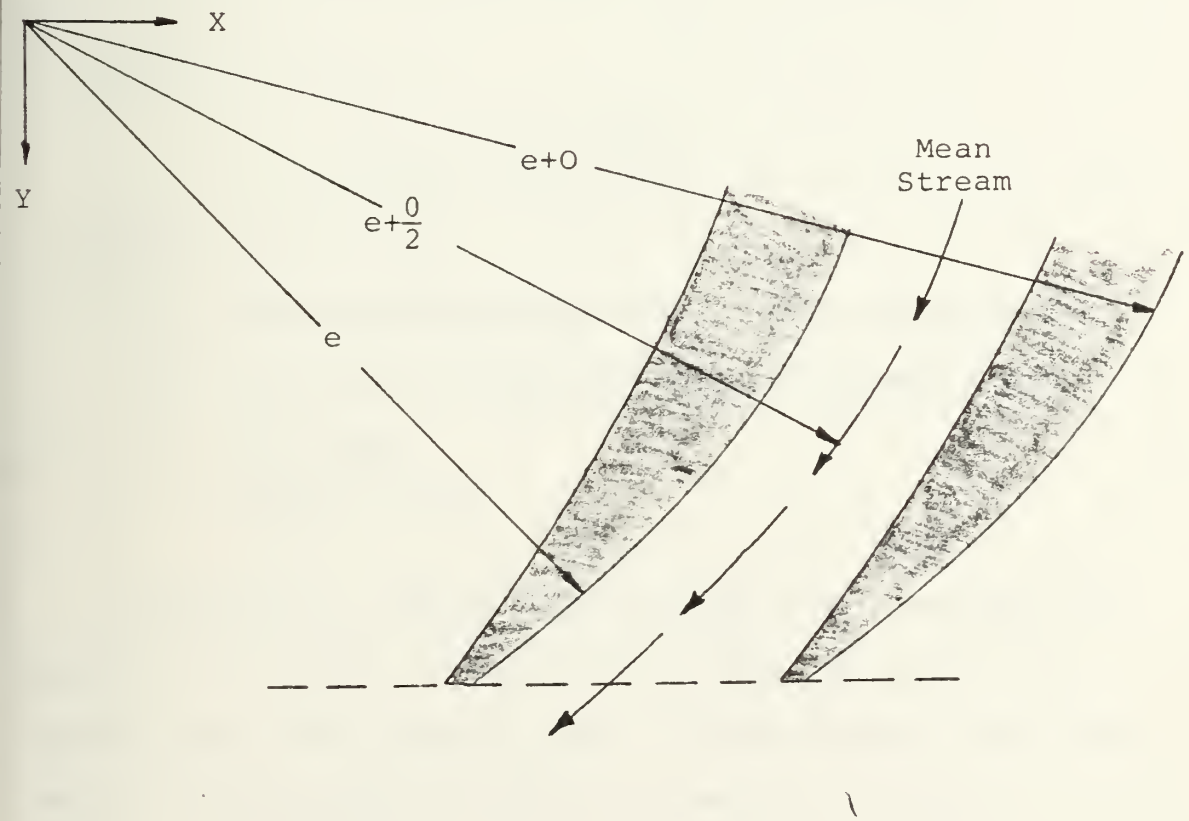

The following method is derived from the aforementioned assumptions and the geometry of figure 9.

For a circle of radius e + o/2;

$$x^2 + y^2 = (e + o/2)^2$$

differentiating,

$$\frac{dy}{dx} = \text{Tan}\,\alpha = \frac{-x}{\left[(e+o/2)^2 - x^2\right]^{\frac{1}{2}}}$$

Now solve for x^2 to get

$$x^2 = \frac{(e + o/2)^2}{1 + \text{Tan}^2\alpha}$$

Finally back substitute above to get

$$y = (e + o/2) \left[1 - \frac{1}{1 + \text{Tan}^2\alpha}\right]^{\frac{1}{2}}$$

and

$$\frac{\Delta b}{b} = \frac{y_{\alpha i} - y_{\alpha' i}}{b_i}$$

where:

$y_{\alpha i}$ = the value of y calculated at original configuration

$y_{\alpha' i}$ = the value of y calculated at modified configuration

b_i = axial chord

i = nozzle or rotor

To determine the tangent of the exit angle it is necessary to account for the change in axial velocity between the leading and trailing edges. This change is due to the fact that the annulus area does not vary precisely with the static density. If a linear

distribution of axial velocity is assumed and an initial guess of 10 percent reduction is made, then the tangents of the exit angles would be

$$\tan \alpha_{exit} = C_\theta / C_{x(reduced)}.$$

Therefore: $\alpha_{exit(R)} = 57.3^\circ$

$\alpha_{exit(N)} = 55.4^\circ$

at mean radius. From the analytical model the percent of change in axial chord can be determined.

$$(\Delta b/b)_{rotor} = 0.081$$

$$(\Delta b/b)_{nozzle} = 0.13$$

Although these estimates for change in axial chord seem reasonable, it is possible that the dynamics involved in such a reduction may rule out such a modification. The dynamic analysis will not be investigated in this paper.

MINIMUM NOZZLE REDUCTION

If it is assumed that the losses due to incidence do not change over a wide range of values, it is possible to find a minimum reduction for the nozzle chord change. This lesser reduction will result in an increased incidence and a higher Mach Number at nozzle exit.

$$\dot{m} = \rho_{st} A_a C_x$$

$$C_x \left[1 - \frac{C_x^2 \left(1 + \mathrm{Tan}^2 \alpha \right)}{2 C_p T_o} \right]^{C_p/R - 1} = \frac{\dot{m} R T_o}{P_o A_a}$$

If the Mach Number at the nozzle exit (M_{NE}) is limited to 0.95 then C_{NE} = 590 m/sec. Since by geometry

$$C_{NE} = \left[C_{x_{NE}}^2 (1 + \tan^2 \alpha)\right]^{\frac{1}{2}}, \text{ from the continuity equation,}$$

$C_{x_{NE}}$ = 316 m/sec. Therefore α_{min} = 57.6° and from the analytical model

$$(\Delta b/b)_{\substack{\text{nozzle} \\ \text{minimum}}} = 0.083$$

This appears advantageous in terms of reduced leaving losses from a large trailing-edge thickness, but calculations of losses using methods and data provided by Wilson and shown in table 10 indicate that increasing the throat Mach Number causes an increase in losses that more than offsets the reduction in losses realized from minimizing the trailing-edge thickness. The estimated efficiency (polytropic, total-total) for the last stage is approximately one percent lower for the minimum-cut nozzle than for the nozzle cut by 13 percent.

This analysis was done for mean-radius chord only. Similar calculations of chord reduction for hub and tip can also be completed, but would have little significant impact.

The concept of cutting back trailing edges is somewhat radical and was investigated from a cost-reduction aspect due to the integrally cast hub and blades. As stated earlier, from a dynamic aspect the conversion may prove to be completely infeasible and a new design may be required. For these reasons a new second-stage blade design is presented (proposal 2) to give the flow directions specified in the velocity diagrams of figure 6. The first-stage blade design was done in a similar manner. Again the method proposed by Wilson was

utilized. Tables 11 through 16 give the blade and nozzle characteristics, and figures 10 through 25 provide the proposed blade shapes.

TABLE 10

NOZZLE AND ROTOR LOSS ESTIMATIONS

	STAGE-ONE		STAGE-TWO				
	NOZZLE REDESIGN	ROTOR REDESIGN	NOZZLE $\frac{\Delta b}{b}=.13$	NOZZLE $\frac{\Delta b}{b}=.085$	NOZZLE REDESIGN	ROTOR $\frac{\Delta b}{b}=.081$	ROTOR REDESIGN
s/b	1.187	.8205	1.128	1.072	.9813	1.0655	.9792
C_L^*	11.5	12.5	12.2	12.3	12.2	9.8	9.9
$C_L^*(s/b)$	13.65	10.25	13.76	13.19	11.97	10.44	9.69
$1-\frac{\cos\alpha_2}{\cos\alpha_1}$	.483	.395	.420	.443	.420	.453	.453
cont. ratio	1.55	1.42	1.45	1.50	1.45	1.50	1.50
$x_{pro}(s/b)\cos\alpha_{out}$	.040	.017	.041	.035	.029	.018	.014
x_{pro}	.0652	.0362	.0644	.0608	.0515	.031	.026
$x_{pro,te}/x_{pro}$	1.17	1.17	1.58	1.50	1.15	1.35	1.15
t_{te}/s	.05	.05	.1494	.1287	.05	.1125	.05
ΔX pro,te	.0003	.0003	.003	.003	.0003	.0015	.0003
h/b	1.25	1.56	2.51	2.38	2.18	3.44	3.16
C_{NE}; w_2 (m/s)	590	576	471	590	472	511	514
O (m)	.01193	.00876	.0094	.00936	.0108	.0083	.00894
M_{throat}	.865	.88	.733	.94	.73	.86	.83
$\gamma'_{st,exit}(10^{-5})$	16.7	14.7	13.8	13.0	13.8	10.9	10.9
Re (10^4)	4.21	3.43	3.20	4.25	3.70	3.89	4.22
X_{sec}	.02	.025	.011	.011	.011	.011	.011
$X_{Re}/X_{Re=10^5}$	1.2	1.3	1.2	1.25	1.12	1.12	1.10
$X_{pro,corrected}$	.092	.0554	.125	.117	.0666	.0484	.0332
ΣX	.112	.0804	.136	.128	.0776	.0594	.0442
q_2 (kPa)	75.3	77.2	31.8	46.3	31.6	40.7	38.6
ΔPo (kPa)	8.43	6.21	4.33	5.93	2.45	2.42	1.71

TABLE 11

REDESIGNED-CONFIGURATION STAGE-ONE

NOZZLE AND ROTOR CHARACTERISTICS

(MEAN RADIUS)

	Rotor (mm)	Nozzle (mm)
r	91.95	84.33
z	36	22
s	16.05	24.10
b	19.56	20.0
M_{throat}	0.88	0.865
s/e	0.5	0.5
o/s	0.545	0.495
Δt_{te}	0.803	1.205
e	32.10	48.20
o	8.76	11.93
c	21.63	27.14

FIGURE 10

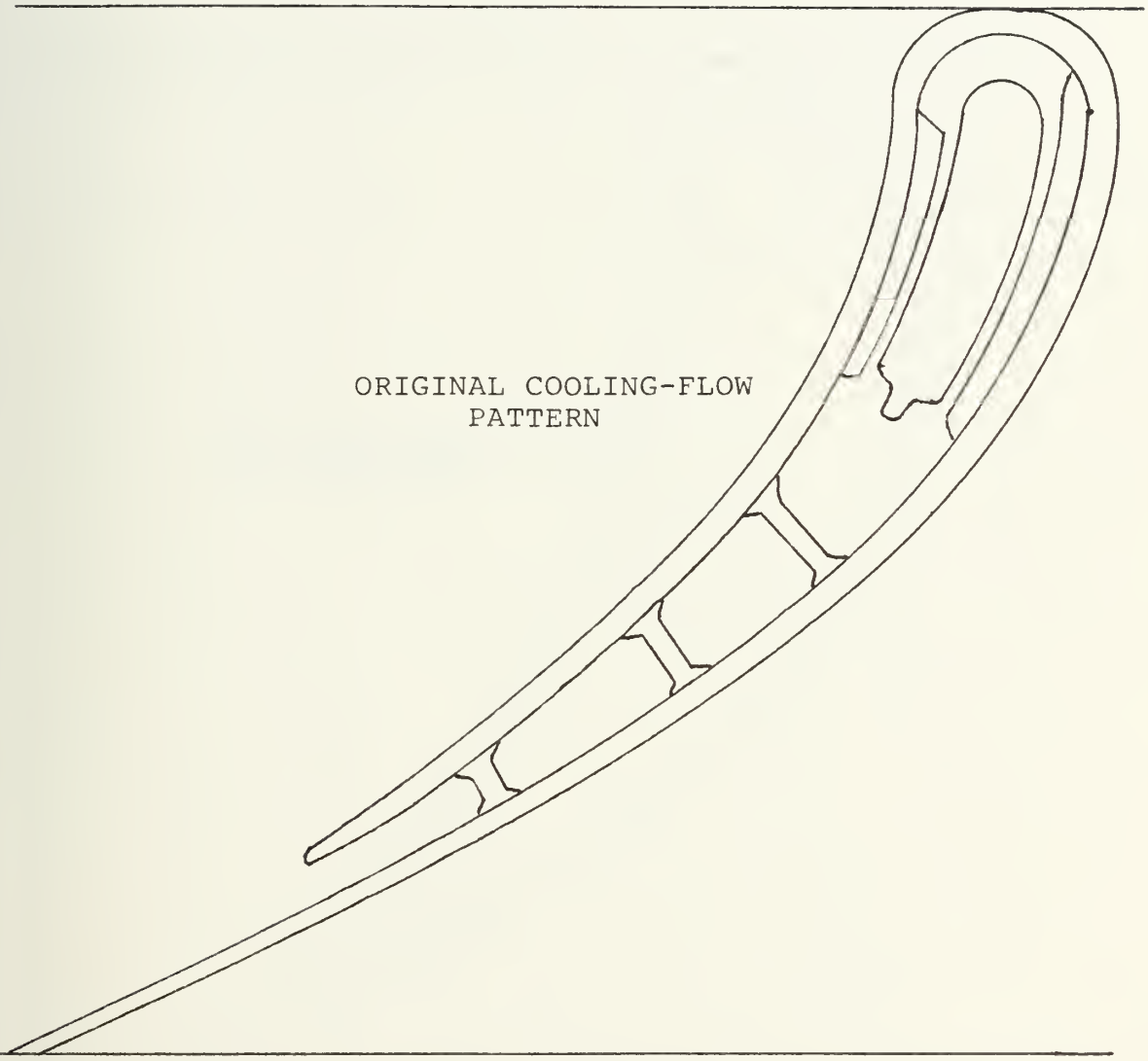

REDESIGNED CONFIGURATION STAGE - ONE NOZZLE (MEAN)

SCALE 7:1

FIGURE 11

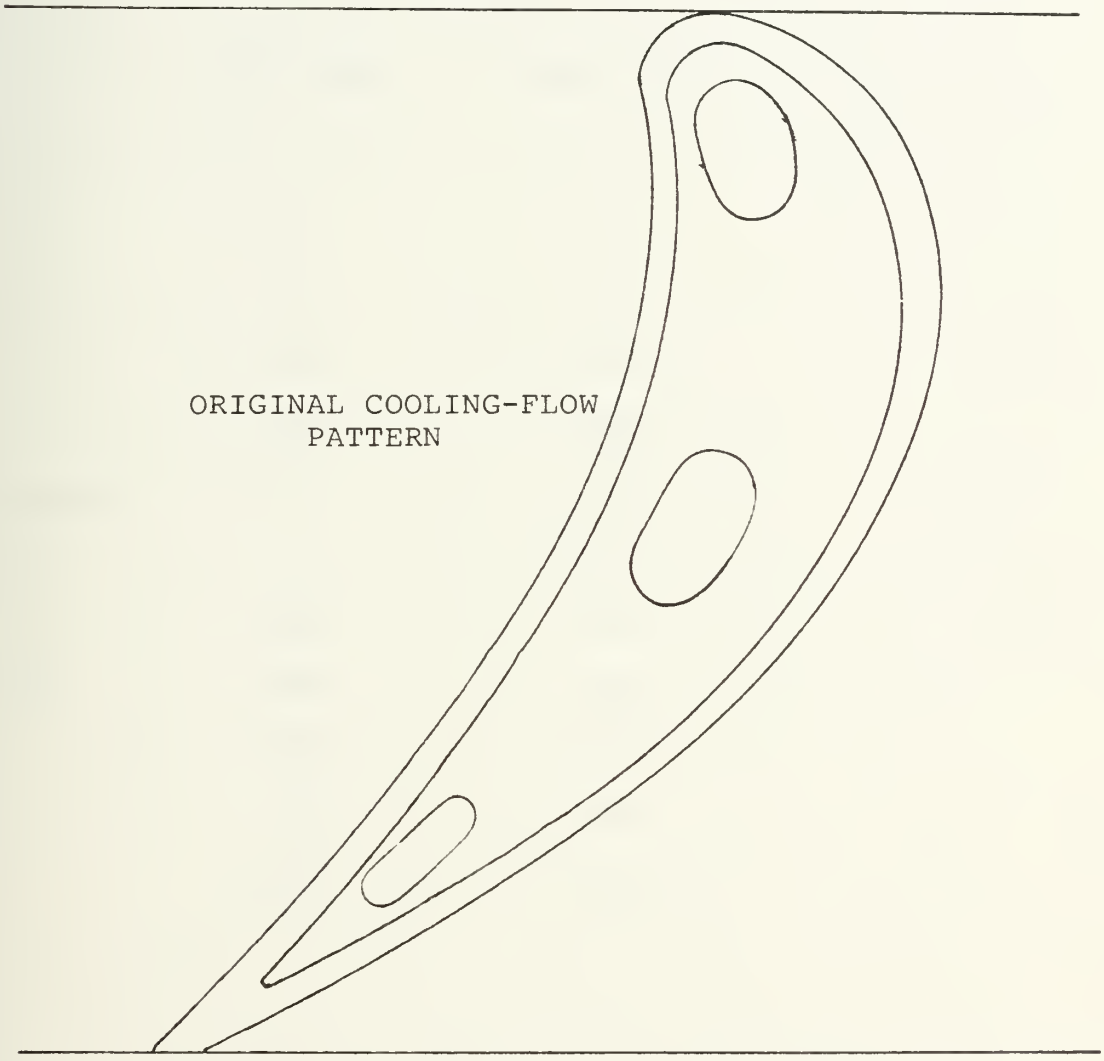

REDESIGNED CONFIGURATION STAGE - ONE ROTOR (MEAN)
SCALE 7:1

TABLE 12

REDESIGNED-CONFIGURATION STAGE-ONE

NOZZLE AND ROTOR CHARACTERISTICS

(HUB)

	Rotor (mm)	Nozzle (mm)
r	74.17	74.17
z	36	22
s	12.95	21.18
b	23.88	18.29
M_{throat}	0.81	1.05
s/e	0.5	0.5
o/s	0.596	0.411
Δt_{te}	0.803	1.205
e	25.90	42.36
o	7.72	8.70
c	25.40	25.40

FIGURE 12

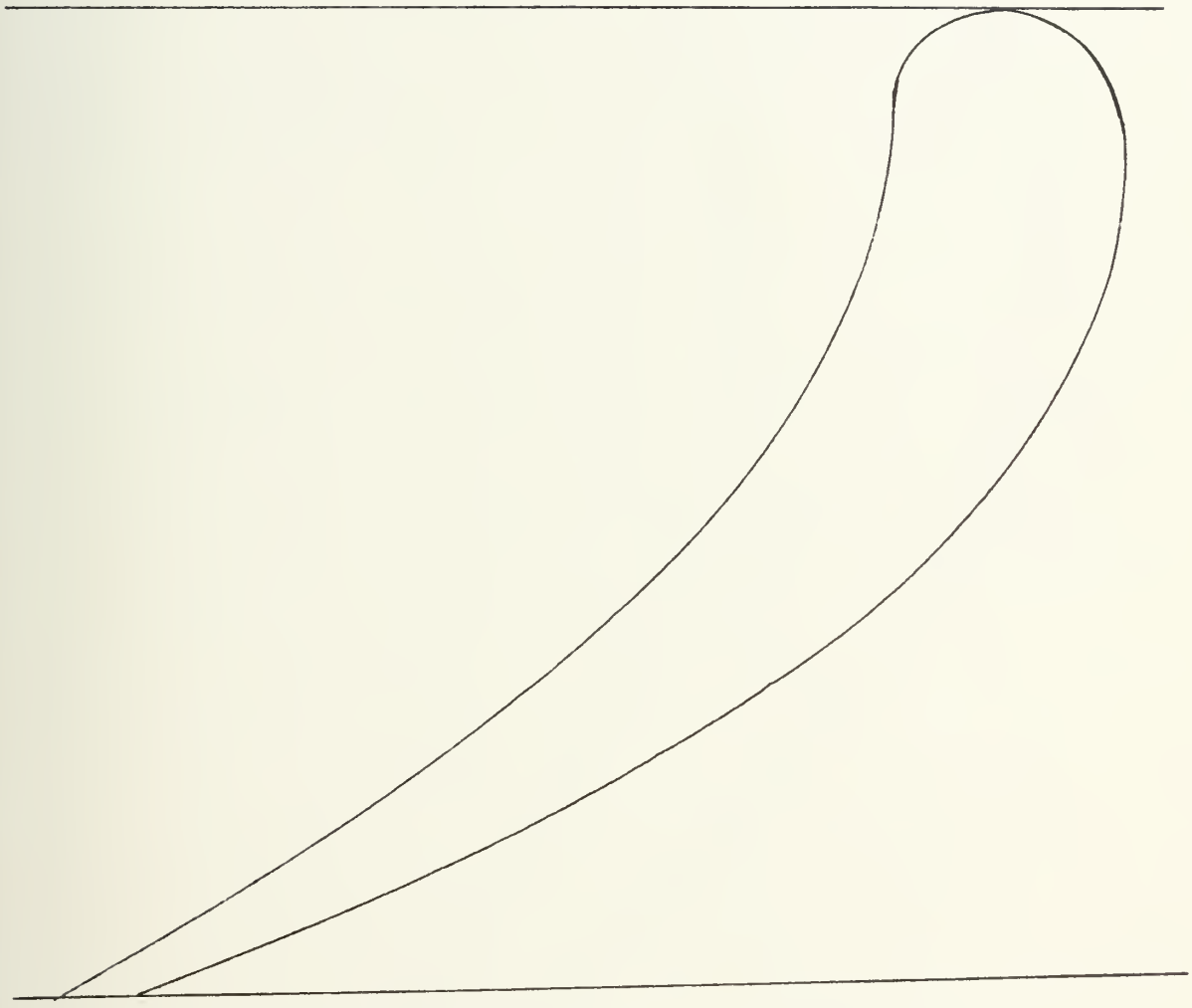

REDESIGNED CONFIGURATION STAGE - ONE NOZZLE (HUB)

SCALE 7:1

FIGURE 13

REDESIGNED CONFIGURATION STAGE - ONE ROTOR (HUB)
SCALE 7:1

TABLE 13

REDESIGNED-CONFIGURATION STAGE-ONE

NOZZLE AND ROTOR CHARACTERISTICS

(TIP)

	Rotor (mm)	Nozzle (mm)
r	21.10	95.50
z	36	22
s	17.82	27.30
b	15.75	22.86
M_{throat}	0.96	0.80
s/e	0.5	0.5
o/s	0.5	0.537
Δt_{te}	0.803	1.205
e	35.64	54.60
o	8.91	14.66
c	19.09	30.12

FIGURE 14

REDESIGNED CONFIGURATION STAGE - ONE NOZZLE (TIP)

SCALE 7:1

FIGURE 15

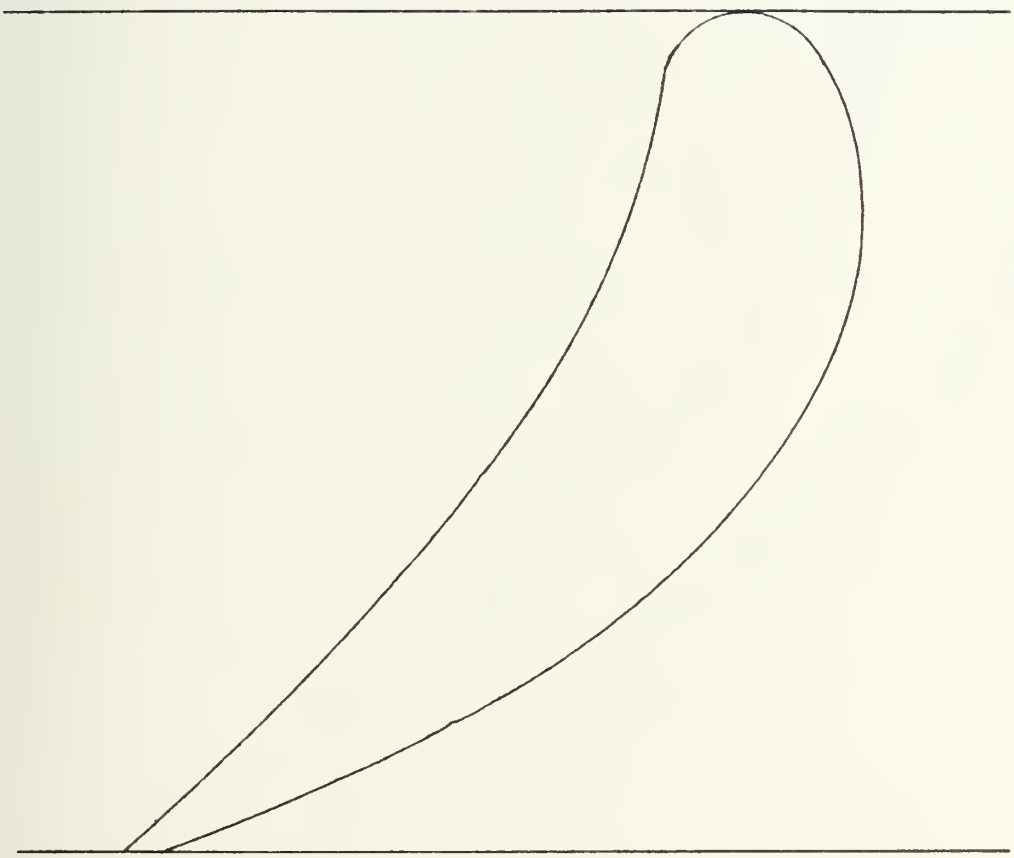

REDESIGNED CONFIGURATION STAGE - ONE ROTOR (TIP)
SCALE 7:1

FIGURE 16

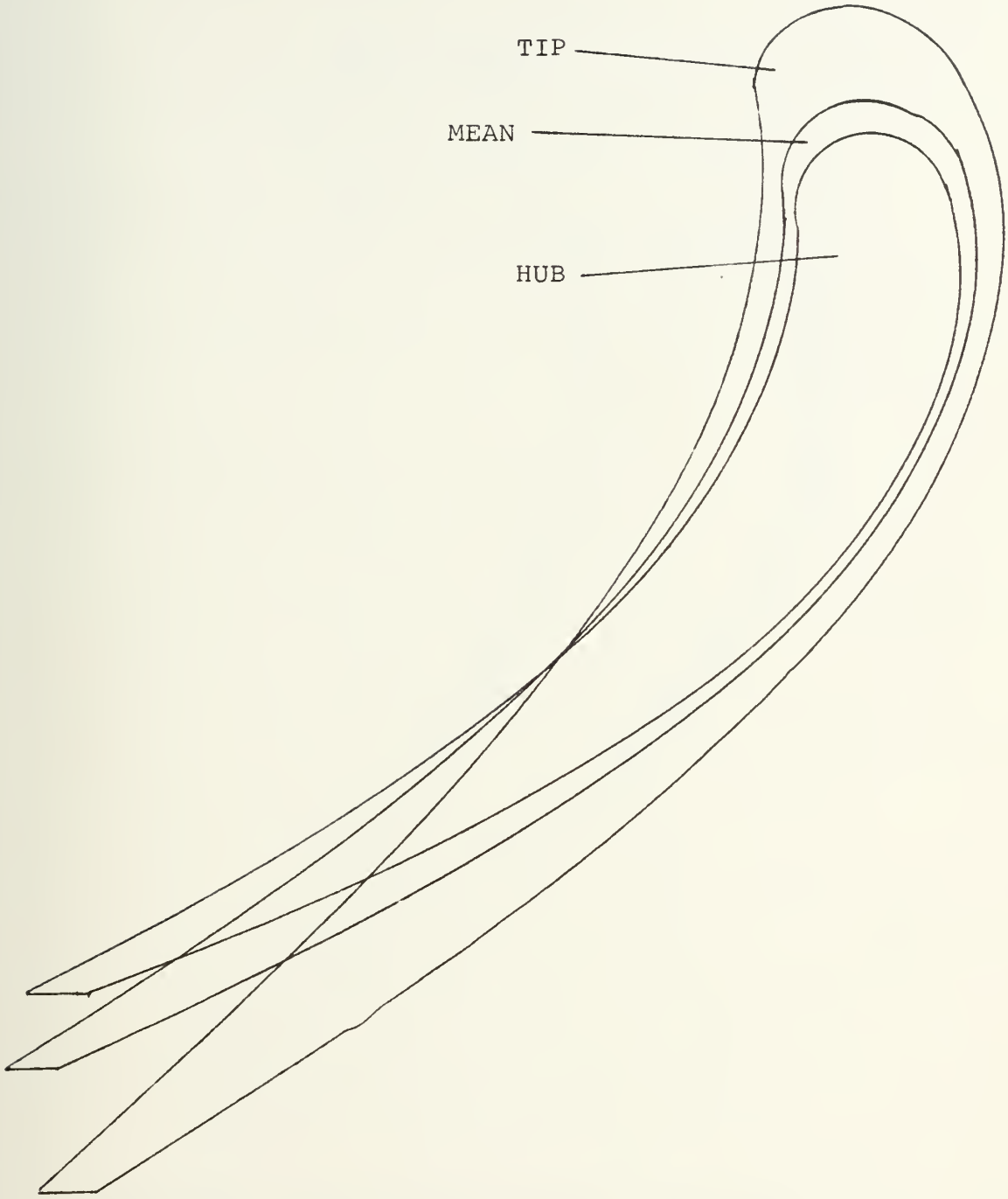

REDESIGNED CONFIGURATION STAGE - ONE NOZZLE
HUB - TIP - MEAN
SCALE 7:1

FIGURE 17

REDESIGNED CONFIGURATION STAGE - ONE ROTOR
HUB - TIP - MEAN
SCALE 7:1

TABLE 14

REDESIGNED-CONFIGURATION STAGE-TWO

NOZZLE AND ROTOR CHARACTERISTICS

(MEAN RADIUS)

	Rotor (mm)	Nozzle (mm)
r	97.05	95.85
z	36	31
s	16.94	19.43
b	17.30	19.80
M_{throat}	0.83	0.73
s/e	0.425	0.5
o/s	0.530	0.555
Δt_{te}	0.847	0.97
e	39.90	38.90
o	8.94	10.80
c	21.20	24.30

FIGURE 18

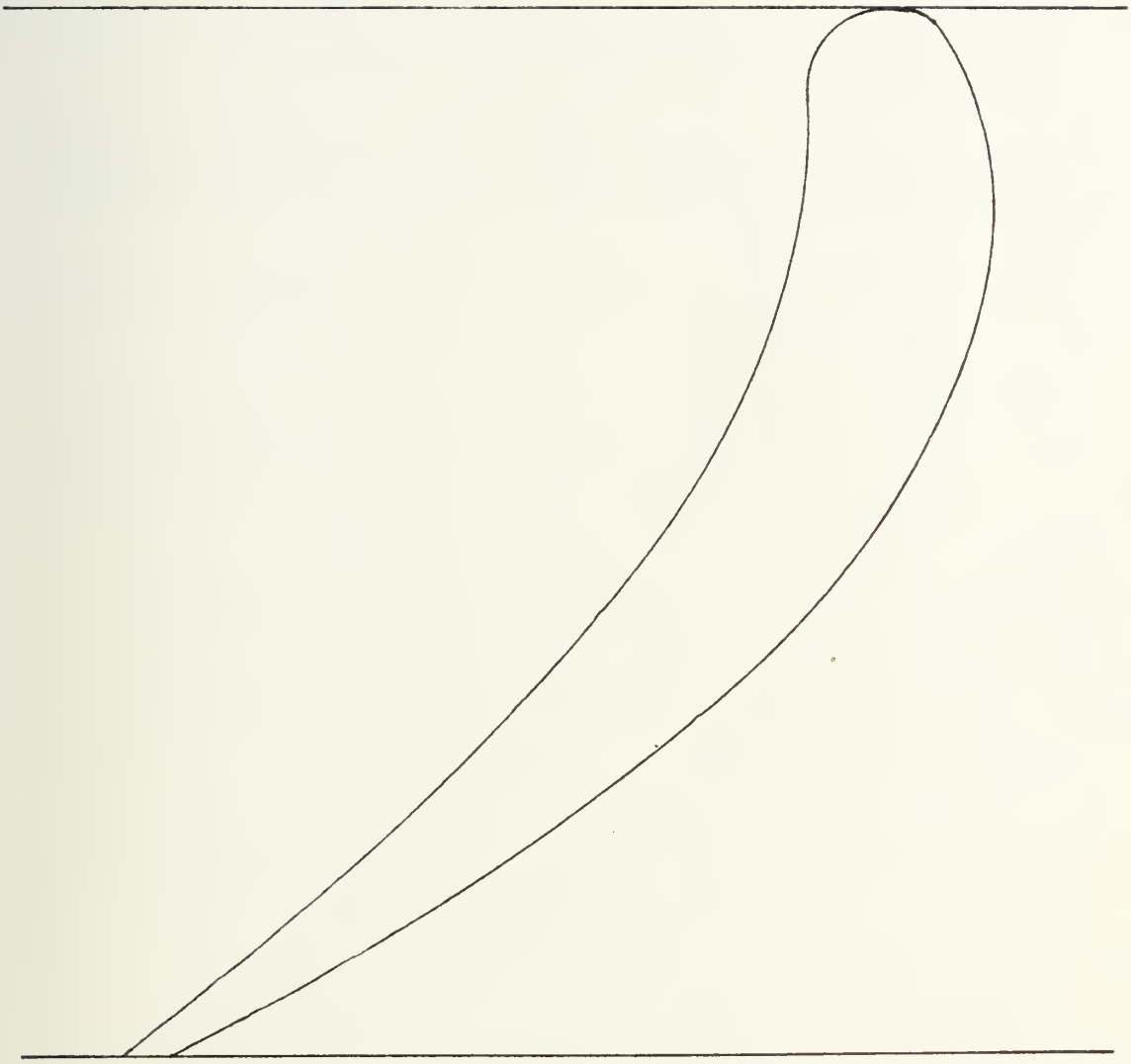

REDESIGNED CONFIGURATION STAGE - TWO NOZZLE (MEAN)

SCALE 7:1

FIGURE 19

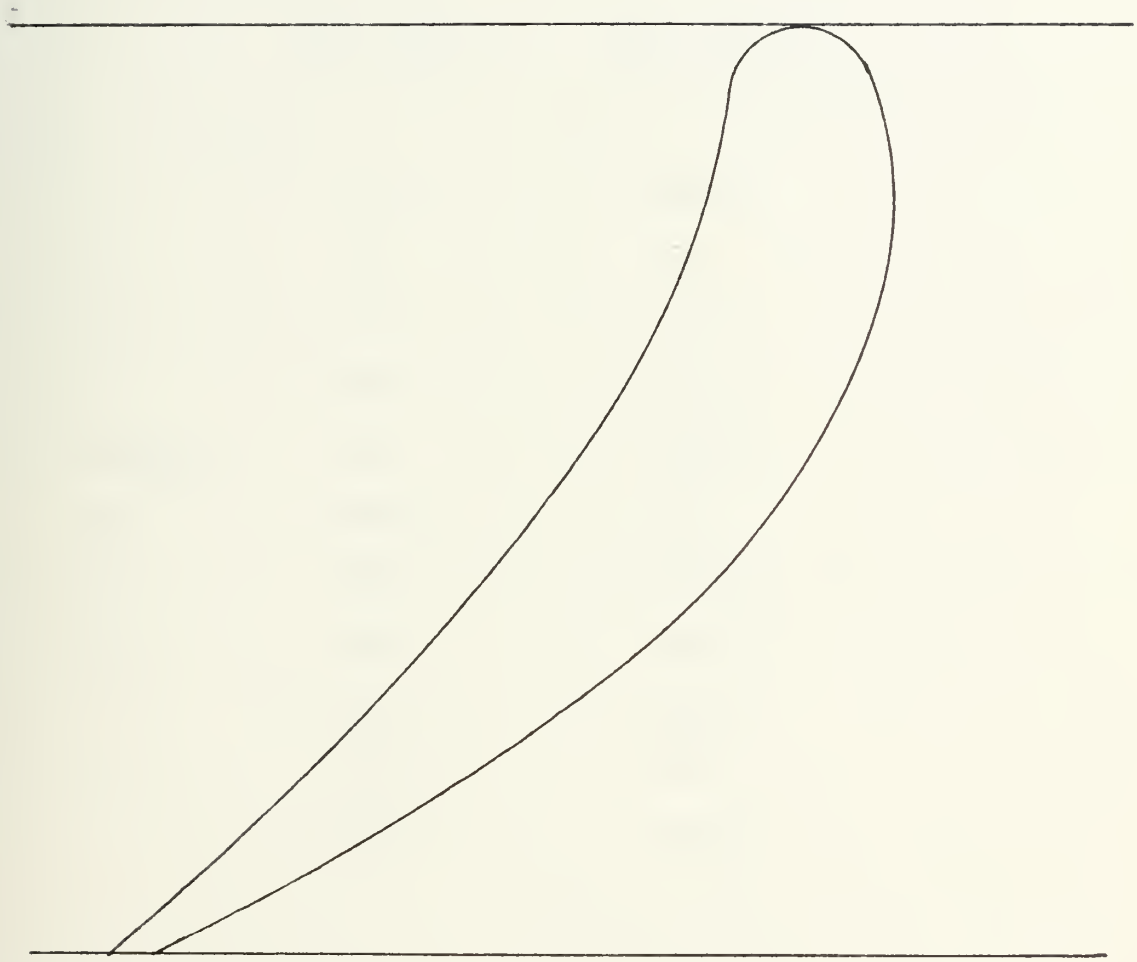

REDESIGNED CONFIGURATION STAGE - TWO ROTOR (MEAN)

SCALE 7:1

TABLE 15

REDESIGNED-CONFIGURATION STAGE-TWO

NOZZLE AND ROTOR CHARACTERISTICS

(HUB)

	Rotor (mm)	Nozzle (mm)
r	71.10	69.60
z	36	31
s	12.41	14.11
b	24.4	16.26
M_{throat}	0.67	0.95
s/e	0.425	0.5
o/s	0.658	0.432
Δt_{te}	0.847	0.97
e	29.20	28.20
o	8.17	6.10
c	25.40	21.05

FIGURE 20

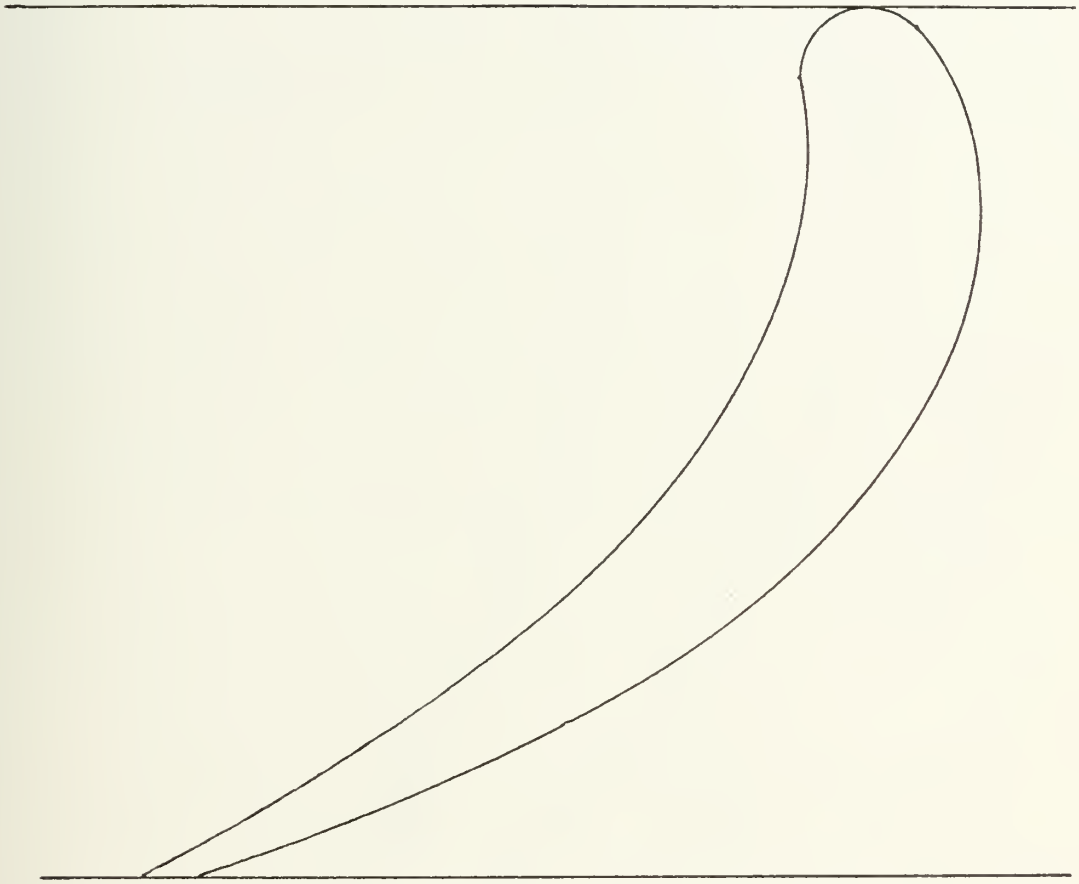

REDESIGNED CONFIGURATION STAGE - TWO NOZZLE (HUB)
SCALE 7:1

FIGURE 21

REDESIGNED CONFIGURATION STAGE - TWO ROTOR (HUB)

SCALE 7:1

TABLE 16

REDESIGNED-CONFIGURATION STAGE-TWO

NOZZLE AND ROTOR CHARACTERISTICS

(TIP)

	Rotor (mm)	Nozzle (mm)
r	123.0	117.0
z	36	31
s	21.50	23.7
b	10.20	24.9
M_{throat}	0.96	0.615
s/e	0.425	0.5
o/s	0.435	0.652
Δt_{te}	0.847	0.97
e	50.60	47.4
o	9.35	14.0
c	16.55	30.30

FIGURE 22

REDESIGNED CONFIGURATION STAGE - TWO NOZZLE (TIP)
SCALE 7:1

FIGURE 23

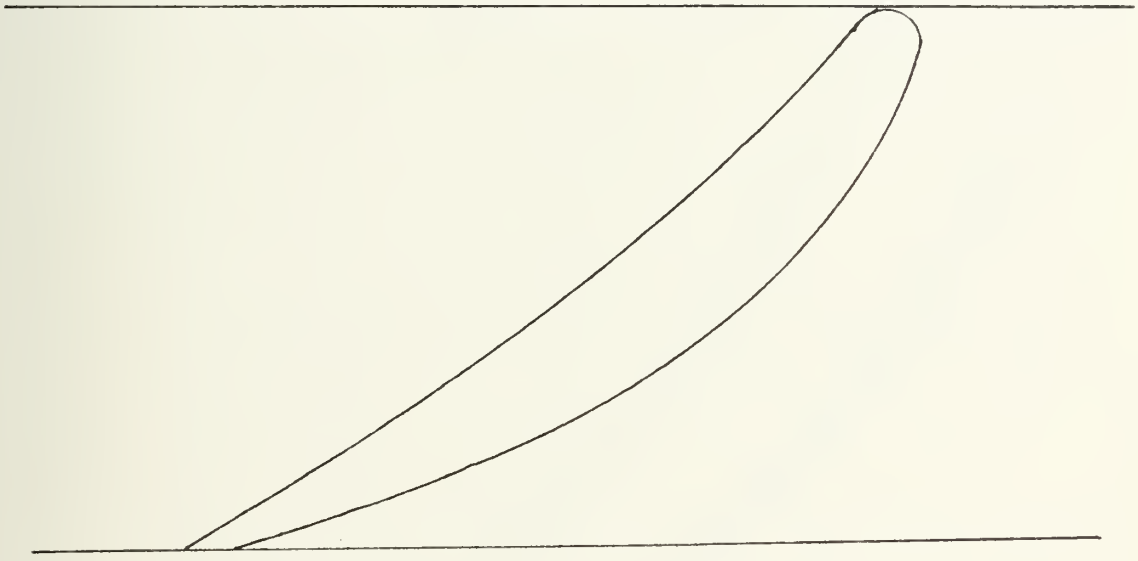

REDESIGNED CONFIGURATION STAGE - TWO ROTOR (TIP)
SCALE 7:1

FIGURE 24

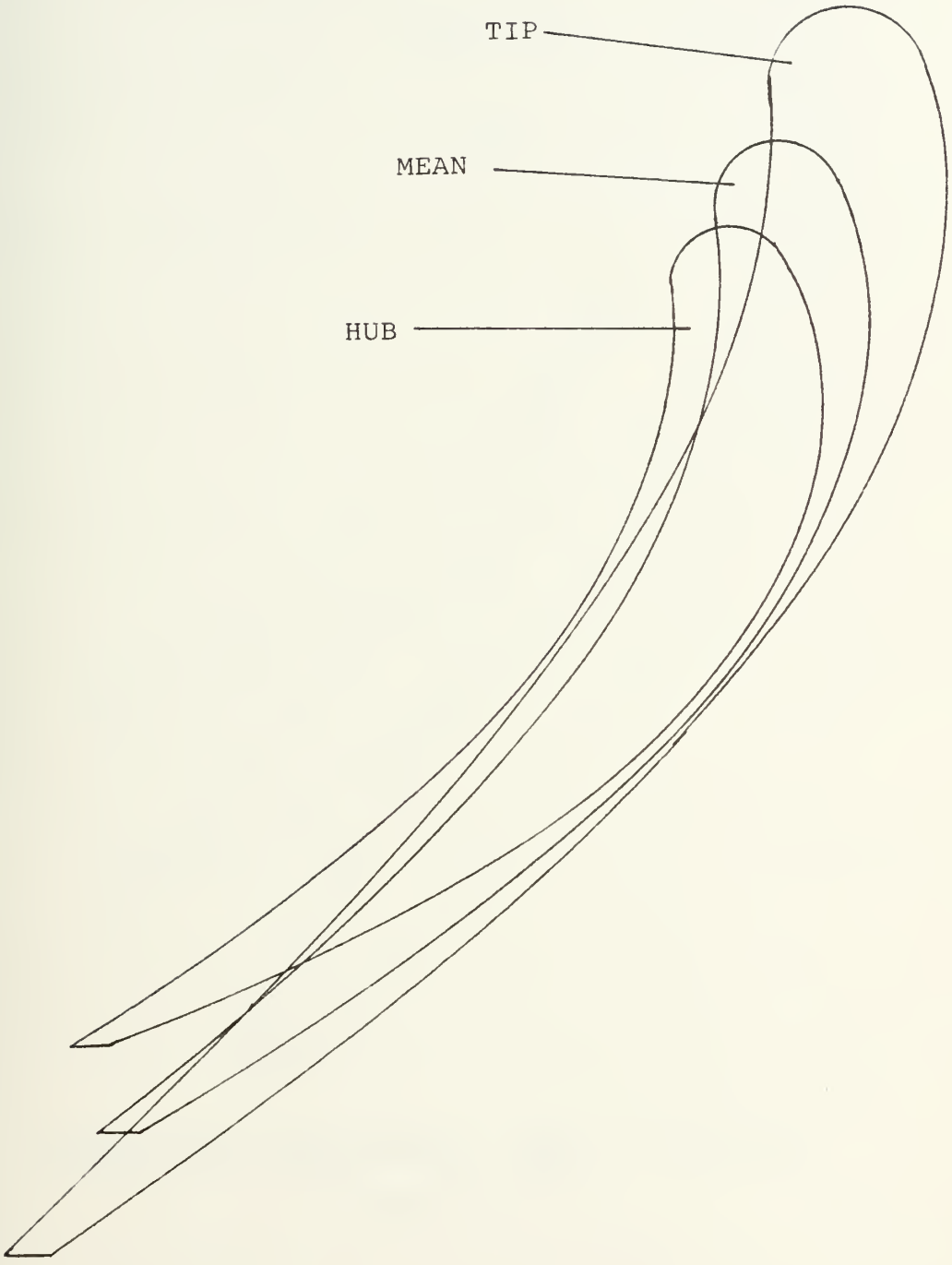

REDESIGNED CONFIGURATION STAGE - TWO NOZZLE
HUB - TIP - MEAN

SCALE 7:1

FIGURE 25

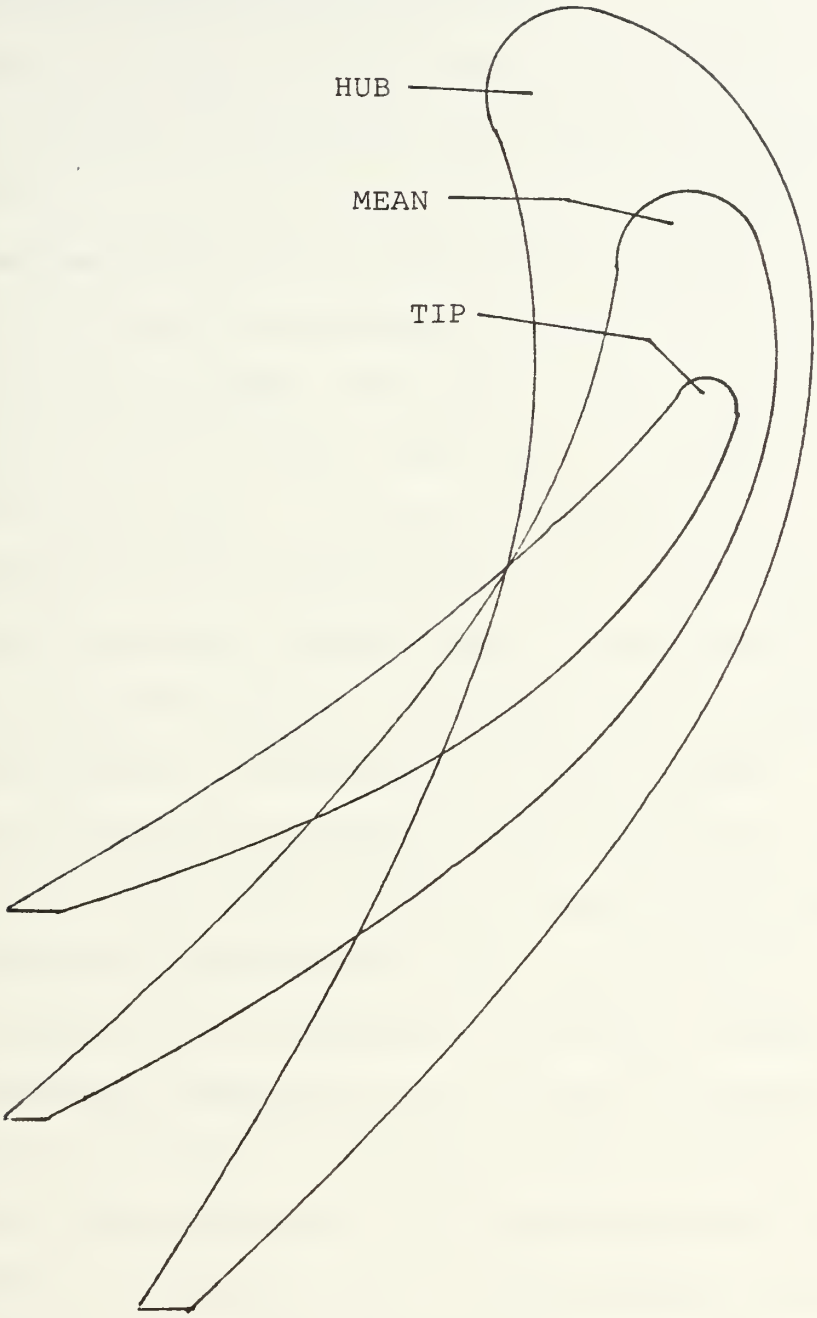

REDESIGNED CONFIGURATION STAGE - TWO ROTOR
HUB - TIP - MEAN
SCALE 7:1

DISCUSSION OF LOSS CALCULATIONS AND EFFICIENCIES

The assumed first-stage polytropic total-total efficiency of 92 percent based on plots of flow and work coefficients given by both Wilson and Horlock (3,6) could be achieved only if a new cooling pattern were developed allowing for optimum conditions of axial chord. The efficiency calculated from the estimated losses is significantly lower than that which was assumed. This lower efficiency should have been anticipated since the principal dimensions of the original first stage (η_p = 0.835) were used. As previously discussed, the original-configuration first-stage dimensions (axial chord) were utilized so that the existing blade and nozzle cooling-patterns could be retained in the modified engine. The increase in efficiency over the original configuration is attributed to the more favorable combination of flow and work coefficients, as was anticipated. No iteration was made to recalculate the effect of the lower first-stage efficiency. It should be noted that the losses given previously (table 10) are calculated as a percentage of stage outlet dynamic head. The exact method proposed by Wilson calls for the losses of the nozzle and rotor to be taken as a percentage of each individual (nozzle or rotor) outlet dynamic head. The former method was chosen because it tended to give results closer to those predicted by both Horlock and Wilson in curves of efficiency as a function of flow and work coefficients.

The concept of grinding back trailing edges was investigated from a feasibility standpoint in an effort to reduce modification costs. This procedure appears attractive and is an option that needs further investigation. Compromise alternatives such as providing new nozzle blades for the existing rotor with modified trailing edges also exist. However, the reduction in efficiency caused by modifying trailing edges is considerable and may be contrary to design goals.

There appear to be several conversion options available, each trading off cost for performance. The high-cost option includes redesign of first and second stages including new cooling-patterns for first-stage nozzle and rotor. Medium-cost options include a new first stage (with existing cooling pattern), new second-stage nozzles and a modified original-configuration third-stage rotor. The low-cost option also requires a new first stage with existing cooling pattern and modified original-configuration third-stage nozzles and rotors. Table 17 summarizes the estimated stage losses and total-total efficiencies of each option while table 18 states the overall engine losses and total-to-static polytropic efficiencies for each option.

TABLE 17

SUMMARY OF LOSSES

AND

TOTAL-TO-TOTAL STAGE EFFICIENCIES

	STAGE-ONE	STAGE-TWO			
		A	B	C	D
ΔP_o (kPa)	14.64	4.16	4.87	6.75	8.35
$\eta_{se,zero\ clear}$ (%)	90.6	94.3	93.4	90.9	88.8
η_{se} (%)	89.2	92.9	92.0	89.5	87.5
η_{pe} (%)	88.4	92.4	91.4	88.8	86.6

A: Redesigned nozzle and rotor

B: Redesigned nozzle and original configuration stage-three rotor trailing edge reduced 8.1%

C: Original configuration stage-three nozzle trailing edge reduced 13% and rotor reduced 8.1%

D: Original configuration stage-three nozzle trailing edge reduced 8.3% and rotor reduced 8.1%

TABLE 18

SUMMARY OF LOSSES

AND

TOTAL-TO-STATIC TURBINE EFFICIENCIES

		A*	B*	C*	D*
ΔP_o (kPa)		18.8	19.51	21.39	22.99
η_{se}	(%)	89.1	88.8	87.8	87.0
η_{se}(%)		87.8	87.4	86.5	85.6
η_{pe}(%)		86.1	85.6	84.5	83.6

A*: Redesigned stage-one plus configuration A stage-two

B*: Redesigned stage-one plus configuration B stage-two

C*: Redesigned stage-one plus configuration C stage-two

D*: Redesigned stage-one plus configuration D stage-two

IV. ROTARY REGENERATOR

The incorporation of a rotary regenerator in the redesigned engine is a key facet in the overall plan to increase the engine efficiency and give it a competitive edge over diesel engines of comparable power rating. A preliminary design of the required regenerator was accomplished utilizing the NTU method as described by Wilson. The specified regenerator material is a glass ceramic matrix, Corning CERCOR No. T20-38 Code 9461, having thermal and physical properties as enumerated in table 19. This data was generously supplied by Corning.

TABLE 19

REGENERATOR MATRIX PROPERTIES

Passage Packing	1.55×10^{6} passages/sq.m.
Porosity	0.67
Hydraulic Diameter	5.08×10^{-4} m
Heat Transfer Area/Volume	5282 sq.m./cu.m.
Colburn Modulus	2.65/Re
Friction Factor	13.3/Re
Ceramic Specific Heat (740 K)	1.122 kJ/kg-K
(780 K)	1.135 kJ/kg-K
Ceramic Solid Density	2258.3 kg/cu.m.

The properties of the gas streams were taken as constant at the mean temperatures of the hot (780 K) and cold (740 K) sides. We have chosen to specify the ratio of the hot-to-cold-side heat-transfer areas as 3:1, the heat-capacity-rate ratio as 1.0, and the switching rate as 5.0. Additionally, the maximum diameter of the regenerator wheels is 0.7112 meters (28 inches) and the maximum thickness is 0.0762 meters (3.0 inches) due to manufacturing constraints, although larger thicknesses are obtainable by placing two or more disks in series. Therefore the diameters are specified at the maximum obtainable and the thicknesses were left to be calculated, noting that the real limit on the thickness derives from consideration of the core pressure drops, which we would like to keep down to approximately two percent.

Pertinent data on the chosen design are displayed in table 20, and figures 26 and 27 show the exhaust ducting and the regenerator layout.

TABLE 20

REGENERATOR DESIGN DATA

Material	Corning CERCOR
	No. T20-38, Code 9461
Wheel Diameter	0.7112 m.
Thickness	0.12 m.

Pressure Drop (hot)	2.37%
(cold)	0.36%
Carryover Loss	0.8% (of compressor inlet)
Weight (matrix only)	284 Kg
Rotation Rate	18.5 seconds/revolution

The regenerator assembly has been designed to be located in the existing engine room overhead to minimize deck space usage and to improve ease of access to the engine for maintenance, although this arrangement could easily be modified to suit the needs of a particular vessel.

FIGURE 26

EXHAUST GAS DUCTING

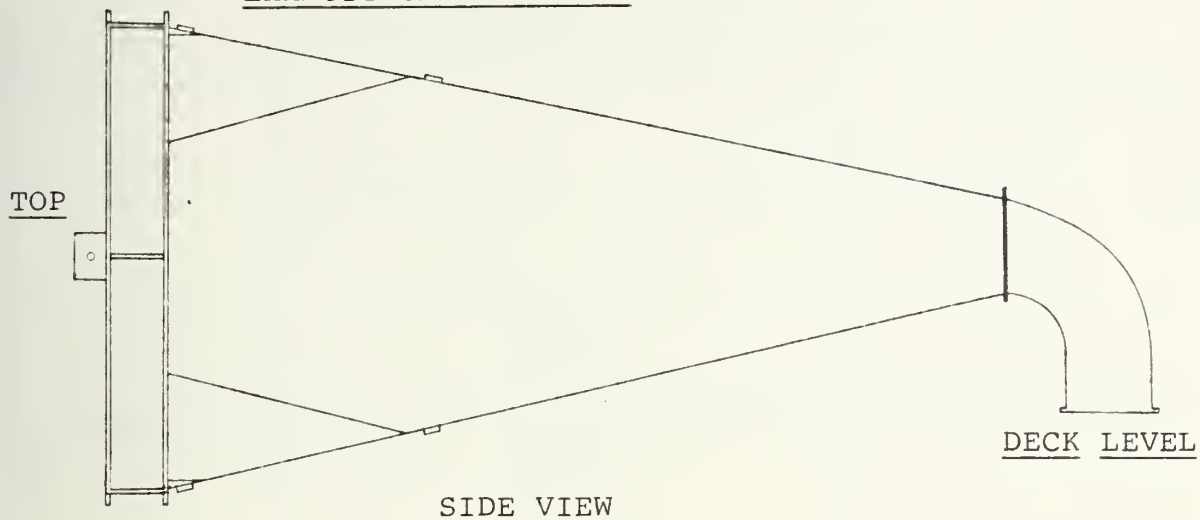

SIDE VIEW
CENTERLINE

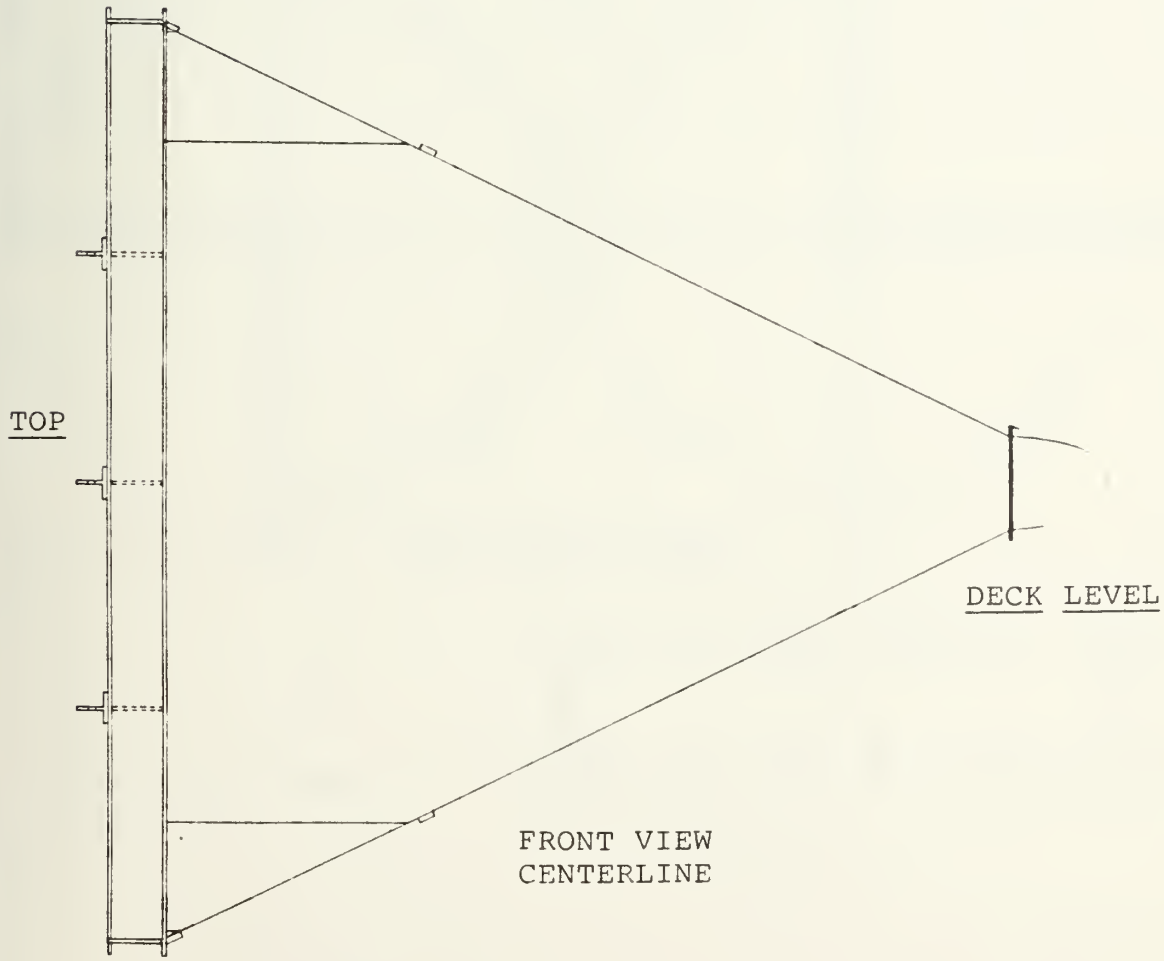

FRONT VIEW
CENTERLINE

FIGURE 27

REGENERATOR HOUSING AND ARRANGEMENT

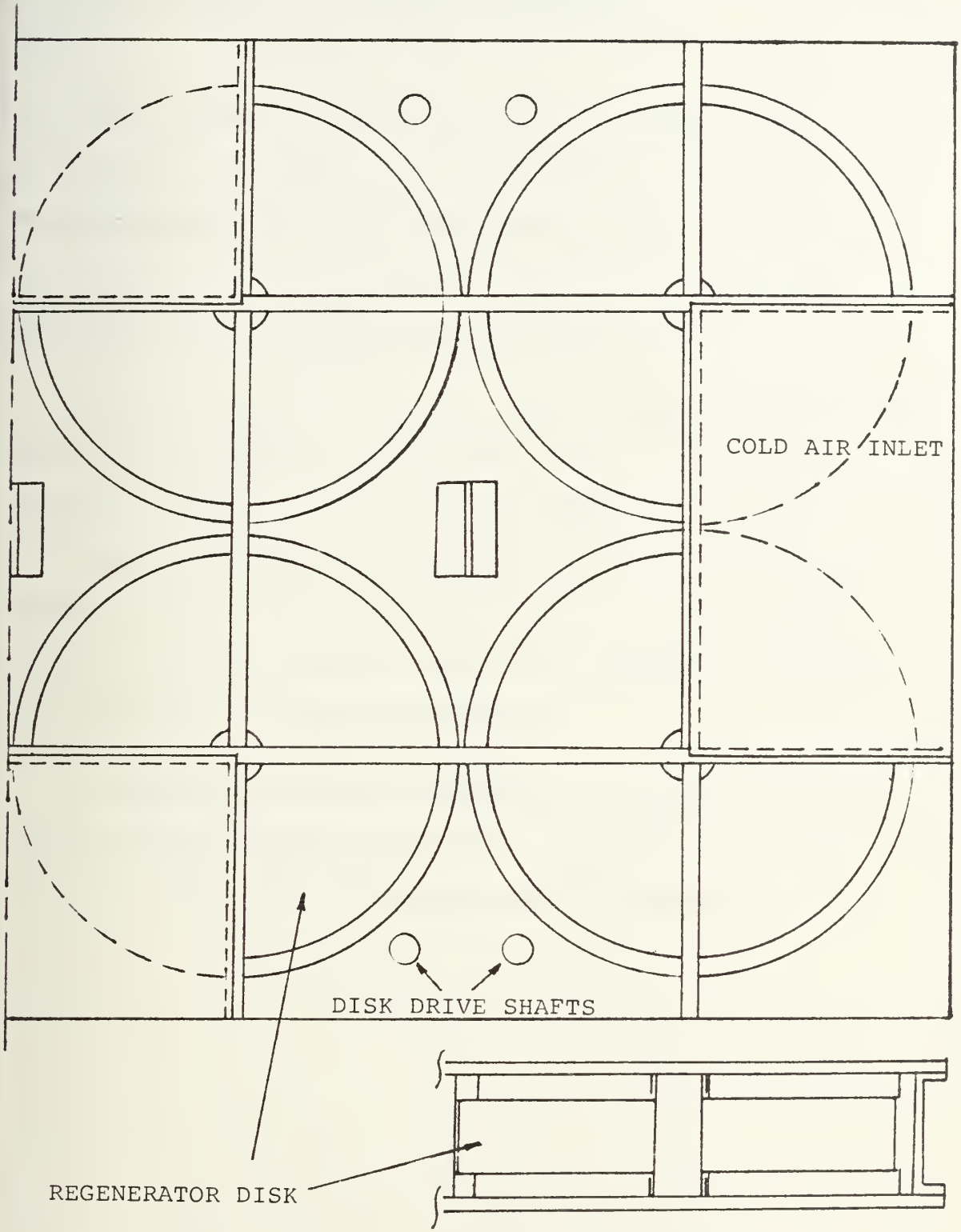

SCALE: 10:1

V. SCROLL AND DUCTING

SCROLL

Since the compressor outlet flow must be directed to the regenerator and returned to the combustor inlet, it was necessary to insert two spiral scrolls that could convert annular to couette flow and vice versa. The actual physical location of the scrolls was selected for ease of insertion into the engine design.

We decided to divide the mass flow and provide two flow paths to and from the regenerator to reduce duct size and to provide some degree of redundancy. A scroll outlet diameter of eighty-nine millimeters (3.5 inches) was selected, resulting in a hot-side return velocity in the duct of 185 m/sec. This is approximately a Mach Number of 0.3 at the combustor inlet scroll (maximum) and provides accelerating flow at the combustor inlet.

The simple scroll design provided here and shown in figure 28 is presented only to show size feasibility. It is based on a linear flow area distribution over a 180 degree angular displacement.

FIGURE 28

SCROLL CROSS - SECTION

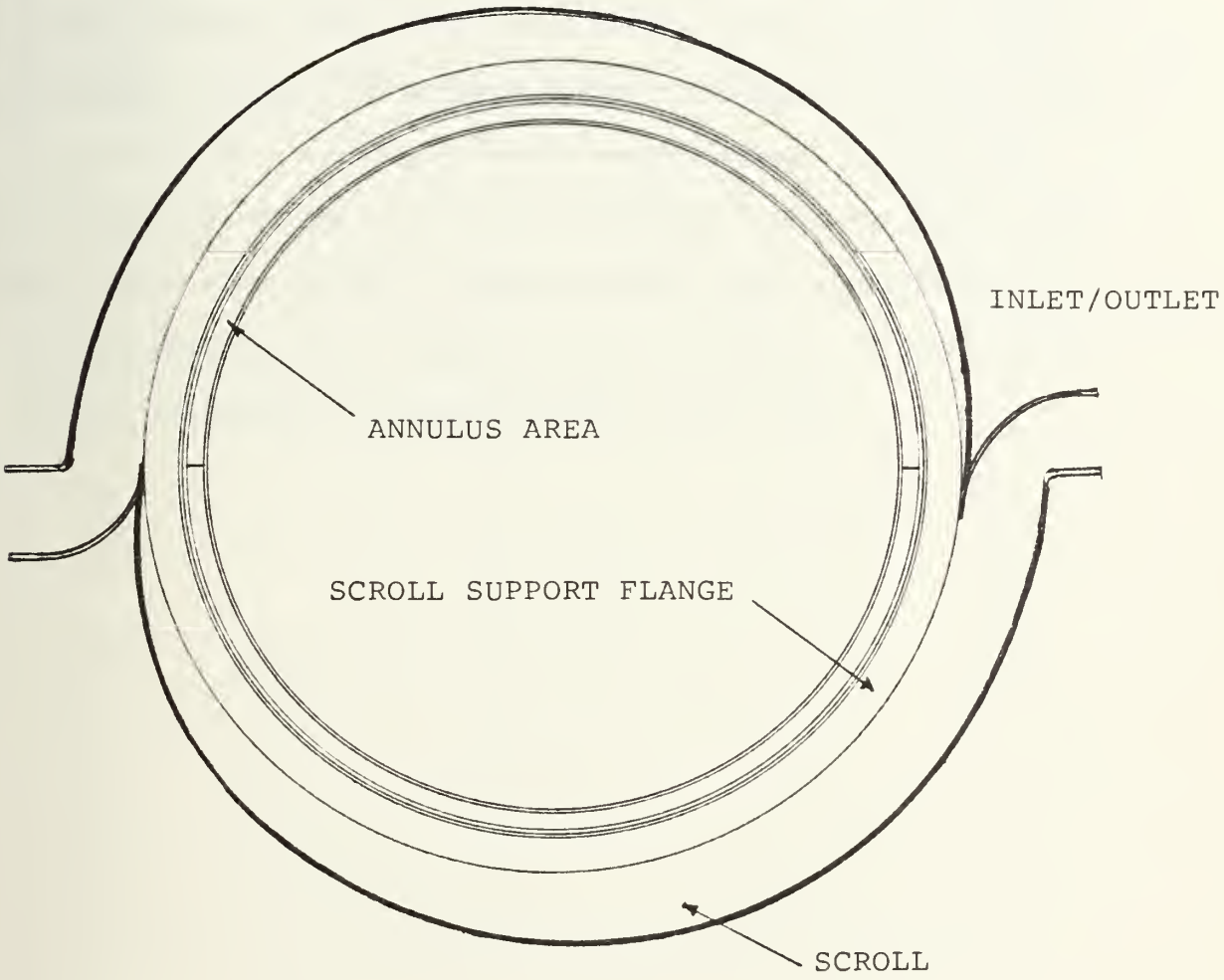

TURBINE EXHAUST DUCTING

The exhaust ducting from the turbine exit to the regenerator was designed primarily for ease of installation on a fishing vessel. The relatively large size of the regenerator assembly requires that the ducting provide a transition from the small turbine exhaust flange (0.3 meter diameter) to the much larger rectangular regenerator face (1.5 m x 3.0 m). A vertical rise of approximately 3.0 meters was selected to allow the system to be installed in the overhead of the main engine room, thereby reducing the deck space required for the on-board modification. Figure 29 shows the general layout of the turbine, exhaust duct, regenerator, and stack inlet.

FIGURE 29

ENGINE - EXHAUST GAS DUCTING - REGENERATOR
GENERAL ARRANGEMENT

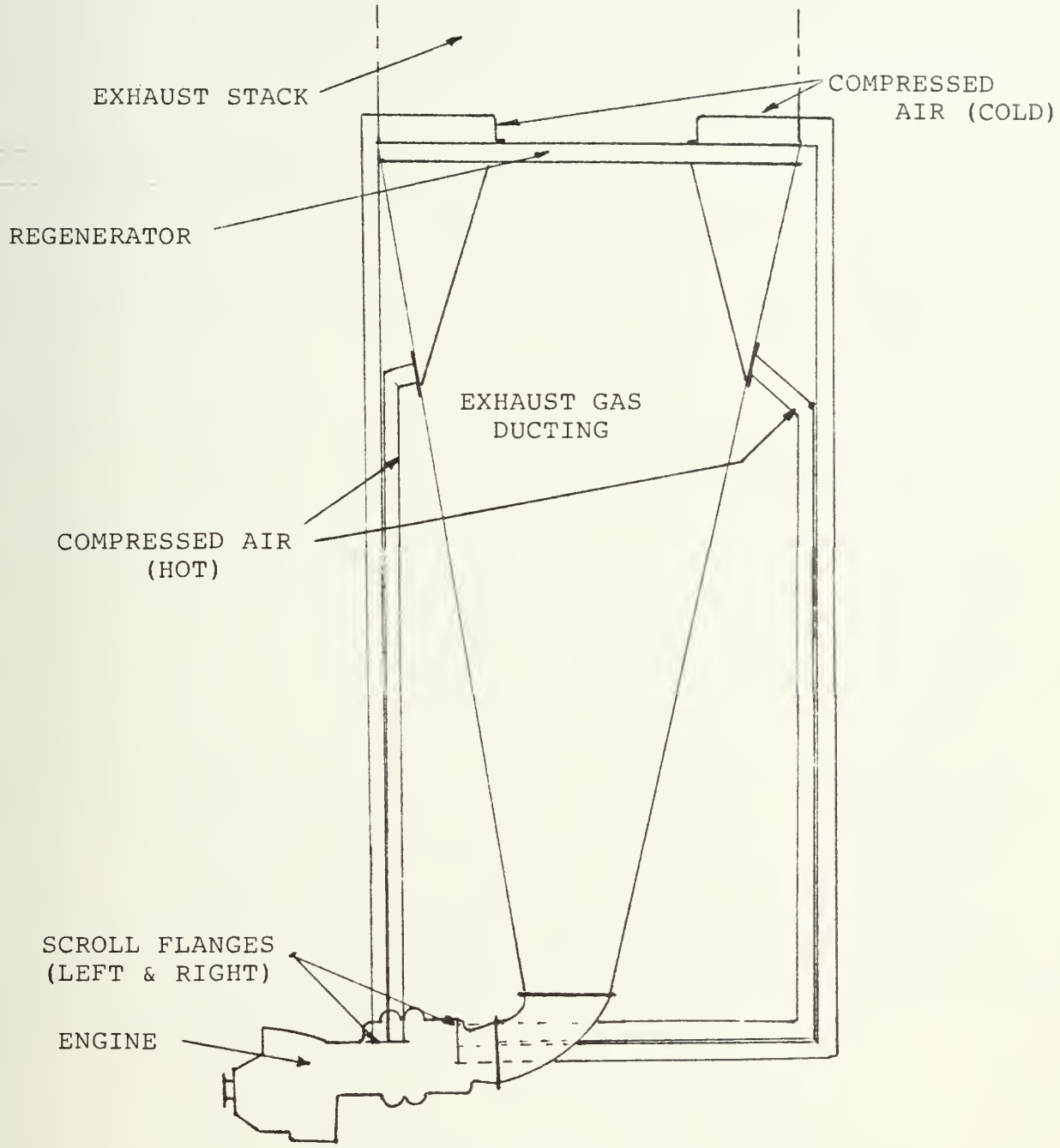

FIGURE 30

REDESIGNED ENGINE CROSS-SECTION

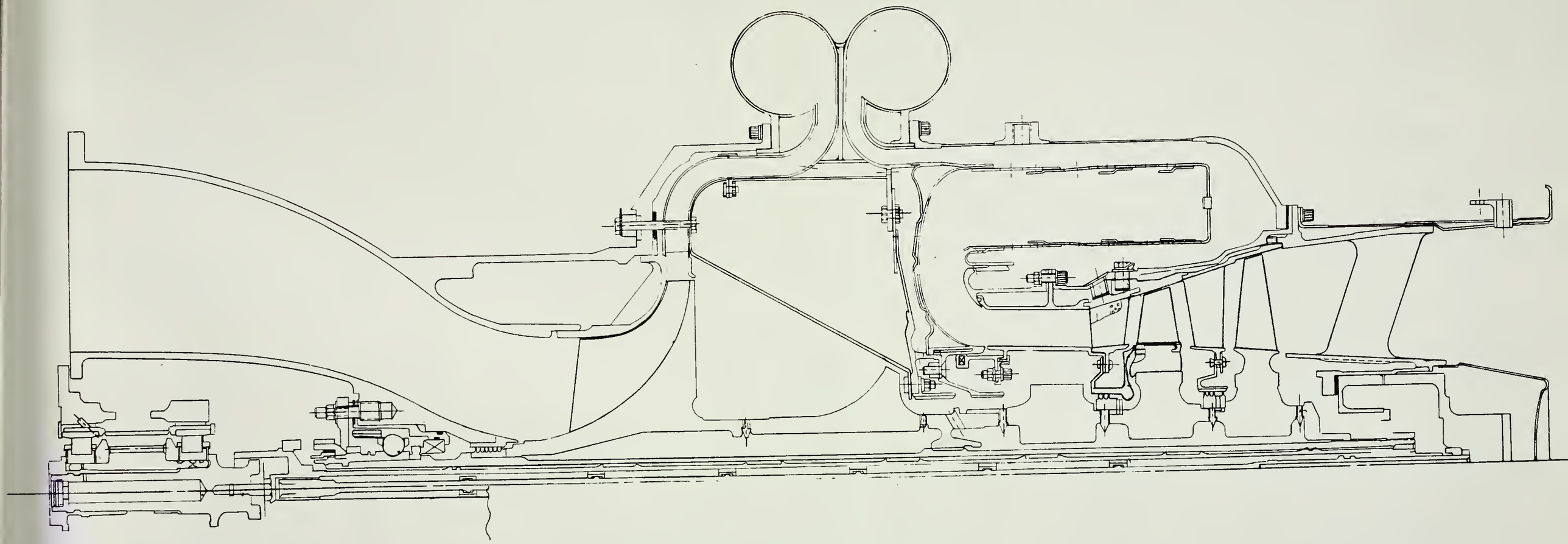

VI. CROSS-SECTION

GENERAL

The modification of the original turbine was accomplished with priority placed on ease of assembly, minimum parts alteration, and minimum parts replacement. Table 21 lists major original equipment parts that are modified and retained. Table 22 lists major equipment parts that will need to be manufactured.

TABLE 21

MODIFIED ORIGINAL EQUIPMENT PARTS

Part	Modification
Second-stage compressor	milled down, blading removed
Second-stage turbine rotor	milled down, blading removed
First-stage hub	none, moved to original second-stage location
Combustor liner	increased jet size

TABLE 22

NEW EQUIPMENT PARTS

Part	Purpose
Primary Support Ring	support, strength member
scroll	exit/inlet flow paths for regenerator
upper annulus ring	defines new first-stage flow area
lower annulus ring	defines new first-stage flow area
nozzle cooling flow pipette	provides nozzle cooling flow
nozzle lower support ring	supports nozzle at hub and directs rotor cooling flow

The effect on the shaft dynamics, although not investigated here, is acknowledged to be considerable and will require further analysis. If such an effort determines that utilization of the milled down second-stage compressor and second-stage turbine hub is not acceptable, then appropriately sized shaft collars could be manufactured and installed.

The cooling passages for both first-stage nozzle and rotor are similar to the original design with one exception; the flow path to the rotor from the compressor outlet is via the original design secondary path through the shaft inner flow area. No back-up flow path was selected. Preliminary analysis of cooling requirements shows that approximately 1.5 percent of the regenerator return flow is required for the first-stage nozzle while 0.5 percent of compressor

outlet flow is needed in the rotor. The large difference between these required cooling flows is due to the large temperature differential between the two sources. For preliminary design purposes the required total cooling flow was taken as 4 percent.

The final redesigned-engine cross-section is depicted in figure 30.

VII. CONCLUSIONS

It was the general purpose of this preliminary redesign to determine the feasibility of a modification program on the selected engine and to identify potential problem areas for further investigation. At the completion of the project no problem areas that would preclude the success of the proposed conversion have been identified and its feasibility seems justifiable. It is felt that the primary influence affecting this result is that of the uncomplicated configuration of the selected engine. Additional factors contributing in a favorable manner were the original engine's oversized combustor design, high-altitude operating environment, and relatively low turbine axial velocity.

The resulting redesigned engine has a power output of approximately 700 kilowatts with a thermal efficiency of 49 percent.

VIII. RECOMMENDATIONS

It is recommended that the design of the proposed modification be carried out in detail. Since the engine, the GARRETT T76-420/421, is itself a modified version of the GARRETT TPE 331 it is recommended that GARRET AIRESEARCH be contracted to conduct a more detailed feasibility and cost analysis for such a conversion.

Although detailed analysis is required for the entire redesign, the following areas are deemed critical and are listed in order of decreasing importance:

(1) the ability of the modified combustor to operate reliably and efficiently;

(2) the effect of utilization of modified original shaft components on the dynamic stability of the machine;

(3) the proposed concept of modifying blade shapes by cutting back trailing edges; and

(4) the sufficiency of the proposed cooling passages and flow rates.

Of these four areas it is felt that only the discovery of adverse rotor dynamic effects could be a limiting consideration in terms of feasibility.

REFERENCES

(1) King, Joseph Adam, "Preliminary Redesign of Existing Gas-Turbine Engines to Incorporate a High-Efficiency, Low-Pressure-Ratio, Highly-Regenerative Cycle for Marine Use," MIT Thesis, MS, Dept. of Aeronautics and Astronautics.

(2) Lefebvre, Arthur W., "Gas Turbine Combustion," Hemisphere Publishing Corp., Washington, D.C., 1983.

(3) Wilson, David Gordon," The Design of High-Efficiency Turbomachinery and Gas Turbines," the MIT Press, Cambridge, MA, 1984.

(4) Gibson, M.M., "The Comparative Performance of Gas Turbine Combustion Chambers," Northern Research and Engineering Corporation Report No. 1064-1, dated January 30, 1963.

(5) Carmichael, A. Douglas, "The Aerodynamic Design of Axial-Flow and Radial-Inflow Turbines," Chap. 4, Sawyer's Gas Turbine Eng. Hdbk., Gas Turbine Publications, Stanford, Conn, 1972.

(6) Horlock, J. H., "Axial Flow Turbines," Krieger Publishing Company, Huntington, New York, 1973.

(7) Dixon, S. L., "Fluid Mechanics, Thermodynamics of Turbomachinery," Pergamon Press, Elmsford, New York, 1979.

(8) Lienhard, John H., "A Heat Transfer Textbook," Prentice-Hall Inc., Englewood, N.J., 1981.